

A Faithful Discretization of the Persistent Homology Transform and Other Topological Transforms

Brittany Terese Fasy^{*†} Samuel Micka[‡] David L. Millman[†] Anna Schenfisch^{*}
Lucia Williams[†]

January 18, 2021

Abstract

Topological descriptors, such as persistence diagrams and Euler characteristic curves, have been shown to be useful for summarizing and differentiating shapes, both empirically and theoretically. One common summary tool is the Persistent Homology Transform (PHT), which represents a shape with a multiset of persistence diagrams parameterized by directions in the ambient space. For practical applicability, we must bound the number of directions needed in order to ensure that the PHT is a faithful representation of a shape. In this work, we provide such a bound for geometric simplicial complexes in arbitrary finite dimension and only general position assumptions (as opposed to bounding curvature). Furthermore, through our choice of proof method, we also provide an algorithm to reconstruct simplicial complexes in arbitrary finite dimension using an oracle to query for augmented persistence diagrams. In the process, we also describe a discretization of other topological transforms, including the Betti Curve Transform and Euler Characteristic Curve Transform.

1 Introduction

Topological Data Analysis (TDA) studies the “shape” of data and is gaining traction in a variety of applications [3, 14, 17, 18, 22, 23, 26, 27]. In particular, TDA extracts information from data by using homological features of shapes (e.g., connected components, loops, k -dimensional voids). These homological features can be summarized using popular descriptors, such as persistence diagrams, which offer insight into the geometry and topology of the original data relative to some specific filtration function.

In [25], Turner et al. defined the *Persistent Homology Transform* (PHT) and *Euler Characteristic Curve Transform* (ECCT), which map a geometric simplicial complex in \mathbb{R}^{d+1} to a family of directional persistence diagrams (and Euler characteristic curves) indexed by directions in \mathbb{S}^d . They showed that the infinite family (parameterized by all of \mathbb{S}^d) is a *faithful* representation of a shape, meaning that no other shape could have generated the same family of directional persistence diagrams. After the PHT and ECCT were shown to be faithful using an infinite set of diagrams or curves, several research groups independently observed that there exists finite faithful representations for various types of simplicial and cubical complexes [1, 4, 8, 13, 21]. In addition, researchers have proposed applications [4, 7, 15, 16, 19, 25] using a sample of this infinite family of diagrams as features in shape analysis pipelines, ignoring the fact that the subsample of directions they chose may not result in a transform that is representative of the shape.

Motivated by the need for a provably faithful discretization of the PHT in applications, Belton et al. gave a faithful discretization of the PHT using only $O(n_0^2)$ (augmented) persistence diagrams for embedded plane graphs with n_0 vertices [1]. To show that this discretization is indeed faithful, Belton et al. used the proof method of *reconstructing* the shape from the set of diagrams. If a shape can be unambiguously reconstructed from a set of diagrams, then the set of diagrams is representative of the shape, i.e., the discretized PHT

^{*}Depart. of Mathematical Sciences, Montana State U.

[†]School of Computing, Montana State U.

[‡]Mathematics & Computer Science Depart. Western Colorado U.

{brittany.fasy, david.millman, annaschenfisch, lucia.williams}@montana.edu {samicka}@western.edu

is faithful. [1] gave the first algorithm for reconstructing embedded graphs in \mathbb{R}^d . This work takes the natural next step of using reconstruction to give the first explicit faithful discretization of the PHT for general simplicial complexes. This method also discretizes any topological transform with certain properties, including the Betti Curve Transform (BCT), and an adaptation of this method discretizes other topological transforms, such as the ECCT.

Note that the setting of reconstruction is more restrictive than theoretically necessary: rather than choosing a finite set of directions to represent a known shape, we begin with no knowledge of the underlying shape, and build up our set of directions constructively using an oracle. While reconstruction is not necessary for choosing a finite set of diagrams to represent a shape, our results show that it is a valuable proof method.

Our Contribution In the current paper, we discretize the PHT and other topological transforms through the lens of reconstruction. That is, we investigate the question: *how can we reconstruct embedded simplicial complexes of arbitrary dimension using a finite number of carefully chosen directional (augmented) persistence diagrams or other topological descriptors?* For clarity of exposition, we focus on persistence diagrams as our main tool of reconstruction. Furthermore, our constructive approach allows us to improve upon the best known solution for oracle-based plane graph reconstruction [2].

The heart of our reconstruction algorithm is a predicate (Algorithm 6) that tests whether or not a set of $k+1$ vertices forms a k -simplex in the unknown simplicial complex. Algorithm 7 gives our main result: an algorithm to reconstruct an unknown simplicial complex from carefully chosen persistence diagrams. Finally, we observe that our reconstruction algorithm, and thus, asymptotic results, apply not just to the PHT, but to any topological transform with certain properties, including the BCT.

2 Background Definitions

In this section, we give an overview of necessary background information, following the notation established in [1, 2]. We assume that the reader is familiar with homology groups (denoted $H_*(\cdot)$) and their Betti numbers (denoted β_*). For a more complete discussion on foundational computational topology, we refer the reader to [5, 10].

2.1 Lower-star Filtrations and Persistence

We define simplicial complexes, lower-star filtrations, and (augmented) persistence diagrams. For a more complete introduction to these topics, see [10].

Simplices and Simplicial Complexes Let $k, d \in \mathbb{N}$. A (*geometric*) k -simplex σ is the convex hull of a set of $k+1$ affinely independent points in \mathbb{R}^d , denoted $\sigma = [v_0, v_1, \dots, v_k]$. Each of these points is called a *vertex*, and we denote the vertex set of σ by $\text{verts}(\sigma)$. We call k the *dimension* of σ , and denote it by $\dim(\sigma)$. For another simplex τ , we say that τ is a *face* of σ and σ is a *coface* of τ if $\emptyset \neq \text{verts}(\tau) \subseteq \text{verts}(\sigma)$; we denote this relation by $\tau \preceq \sigma$. If $\tau \preceq \sigma$ but $\tau \neq \sigma$, then τ is called a *proper face* of σ , denoted by $\tau \prec \sigma$.

A *simplicial complex* K is a finite set of simplices such that for all $\sigma \in K$, the following two conditions hold: (1) if $\tau \preceq \sigma$, then $\tau \in K$; and (2) if $\sigma' \in K$, then $\sigma' \cap \sigma$ is either empty or an element of K . We topologize K with the Alexandroff topology. We denote the set of k -simplices in K by K_k and the number of simplices in K_k by n_k . We let $n = \sum_{k \in \mathbb{N}} n_k$. The *degree* of $v \in K_0$ is the number of one-simplices (edges) that are cofaces of v , and we denote this as $\deg(v)$.

Filtrations and Persistent Homology Next, we introduce a filtered topological space. Let $f: K \rightarrow \mathbb{R}$ be a monotonic function, meaning that for each pair of simplices $\tau \prec \sigma \in K$, we have $f(\tau) \leq f(\sigma)$. Thus, each sublevel set $f^{-1}(-\infty, t]$ with $t \in \mathbb{R}$ is a simplicial complex. Moreover, $f^{-1}(-\infty, t]$ realizes at most $n+1$ distinct complexes: the empty set and $f^{-1}(-\infty, f(\sigma)]$ for each $\sigma \in K$. Let $t_1 < t_2 < \dots < t_\eta$ be the ordered set of minimum function values that realize distinct complexes (we call these *event times*). Letting $F_0 := \emptyset$ and $F_i := f^{-1}(-\infty, t_i]$, the following sequence of nested simplicial complexes is the filtration of K with respect to f :

$$\emptyset = F_0 \subset F_1 \subset F_2 \subset \dots \subset F_\eta = K. \quad (1)$$

Let $k \in \mathbb{N}$. Applying the homology functor to the filtration, we obtain the *persistence module*

$$H_k(F_0) \rightarrow H_k(F_1) \rightarrow H_k(F_2) \rightarrow \dots \rightarrow H_k(F_\eta).$$

Here, we assume that homology is computed using field coefficients (e.g., \mathbb{Z}_2). Then, for each pair of complexes $F_i \subset F_j$ in a filtration, the homology groups $H_k(F_i)$ and $H_k(F_j)$ are vector spaces, and the maps $f_k^{i,j} : H_k(F_i) \rightarrow H_k(F_j)$ are linear maps. Letting $\beta_k^{i,j}$ denote the rank of $f_k^{i,j}$ and $(a, b)^m$ denote m copies of the point (a, b) , we define the k -dimensional persistence diagram, as the following multiset:

$$\mathcal{D}_k(f) := \{(t_i, t_j)^{\mu_k^{(i,j)}} \text{ s.t. } (t_i, t_j) \in \overline{\mathbb{R}}^2 \text{ and } \mu_k^{(i,j)} = \beta_k^{i,j-1} - \beta_k^{i,j} - \beta_k^{i-1,j-1} + \beta_k^{i-1,j}\}.$$

Colloquially speaking, each $(t_i, t_j) \in \mathcal{D}_k(f)$ represents a k -dimensional homological generator $\alpha \in H(F_i)$ such that $[\alpha] \notin \text{im}(f_k^{i-1,i})$ and j is the smallest index such that there exists $[\alpha'] \neq [\alpha] \in H(F_{i-1})$ with $[\alpha] = [\alpha']$ in $H(F_j)$. The *persistence diagram* is the union of all k -dimensional diagrams: $\mathcal{D}(f) := \cup_{k \in \mathbb{Z}} \mathcal{D}_k(f)$.

Lower-Star Filtration In this paper, we are specifically interested in persistence diagrams for *lower-star filtrations* of a simplicial complex $K \subset \mathbb{R}^d$ with respect to a direction $s \in \mathbb{S}^{d-1}$. For each vertex $v \in K_0$, the height of v in direction s is given by the dot product, $s \cdot v$. The lower-star filter function $h_s : K \rightarrow \mathbb{R}$ defines a “height” of each simplex in K where $h_s(\sigma) = \max\{s \cdot v \mid v \in \text{verts}(\sigma)\}$, i.e., $h_s(\sigma)$ is the height of the highest vertex in σ with respect to s . Then the lower-star filtration is the sublevel set filtration of K with respect to h_s . Notice that $h_s^{-1}(-\infty, r] = h_s^{-1}(-\infty, t]$ if and only if no vertex has height in the interval $(r, t]$. If all vertices are at distinct heights, then the total number of distinct subcomplexes (η in the above equations) is $\Theta(n_0)$ and there exists an ordering of the vertices $\{v'_0, v'_1, \dots, v'_{n_0}\}$ such that our filtration is:

$$\emptyset \subset f^{-1}(-\infty, s \cdot v'_0] \subset f^{-1}(-\infty, s \cdot v'_1] \subset \dots \subset f^{-1}(-\infty, s \cdot v'_{n_0}].$$

We now present the main object used in our reconstruction algorithm, the augmented persistence diagram.

Definition 1 (Augmented Persistence Diagram). *Given a filter $f : K \rightarrow \mathbb{R}$, let f' be a compatible index filtration. For $k \in \mathbb{Z}$, the k -dimensional augmented persistence diagram (APD) is defined as the following multiset:*

$$\widehat{\mathcal{D}}_k(f) := \{(f(\sigma_i), f(\sigma_j))\}_{(i,j) \in \mathcal{D}_k(f')}, \quad (2)$$

The APD for f is the union of all k -dimensional augmented diagrams: $\widehat{\mathcal{D}}(f) := \cup_{k \in \mathbb{Z}} \widehat{\mathcal{D}}_k(f)$.

Note that algorithms that compute PDs often find the extra information contained in APDs, but discard it to produce the corresponding PD (see [10]). Additionally, the definition of the PD in related work is often what we defined as the APD (e.g., [20]). Since we will only use APDs in what follows, we use “diagrams” as shorthand for “directional augmented persistence diagrams.”

We also formally define the PHT.

Definition 2 (Persistent Homology Transform). *Given a geometric simplicial complex K in \mathbb{R}^d , the Persistent Homology Transform (PHT) of K is the set of all directional APDs of lower-star filtrations over K , parameterized by the sphere of directions, \mathbb{S}^{d-1} .*

Other transforms are defined similarly, replacing “directional APDs” with the appropriate descriptor (e.g., directional augmented Betti curves or directional augmented Euler characteristic curves).

We note that the results we present rely on knowing heights and dimension of simplices, meaning that the same set of directions that represent the PHT can represent any topological transform that contains this information (e.g., the BCT). Furthermore, by adapting the methods used for edge reconstruction, we can discretize any topological transform that uses directional descriptors that contain the heights and dimensions of simplices (e.g., the BCT), and we call such transforms *dimension-returning transforms*.

However, we proceed using APDs as the main tool of reconstruction. Thus, the definitions of augmented Betti curves and augmented Euler characteristic curves have been placed in Appendix A.2 and Appendix A.3, respectively, and we return to this connection in the conclusion. A proof that APDs, ABCs, and AECCs are well-defined can be found in Appendix A.1.

2.2 Tools for Reconstruction

We now give a lemma that relates simplices to points in an APD, discuss general position assumptions, and define a tool for reconstruction called *filtration hyperplanes*.

Lemma 3 (Simplex Count). *Let K be a simplicial complex. Let $k \in \mathbb{Z}$ and $c \in \mathbb{R}$. Let $f: K \rightarrow \mathbb{R}$ be a monotonic function. Then, the i -dimensional simplices of K are in one-to-one correspondence with the points in the following multiset:*

$$\left\{ (b, d) \in \widehat{\mathcal{D}}_k(f) \text{ s.t. } b = c \right\} \cup \left\{ (b, d) \in \widehat{\mathcal{D}}_{k-1}(f) \text{ s.t. } d = c \right\}. \quad (3)$$

Proof. Let $f': K \rightarrow \mathbb{N}$ be an index filter function compatible with f . Let $\sigma_1, \sigma_2, \dots, \sigma_n$ be the ordering of simplices in K such that $f'(\sigma_i) = i$. Then, the index filtration is $F'_i := f'^{-1}(-\infty, i]$. Consider the sets

$$C_B := \{(i, j) \in \mathcal{D}_k(f') \text{ s.t. } f(\sigma_i) = c\} \quad C_D := \{(i, j) \in \mathcal{D}_{k-1}(f') \text{ s.t. } f(\sigma_j) = c\}$$

and let $C = C_B \cup C_D$. We start by defining a bijection $\phi: f^{-1}(c) \rightarrow C$, and then we compose ϕ with a function from $\mathcal{D}_k(f')$ to $\widehat{\mathcal{D}}_k(f)$ in order to arrive at the desired correspondence.

Let $\sigma_i \in K_k$ such that $f(\sigma_i) = c$. Then, either $\beta_k(F'_i) = \beta_k(F'_i) + 1$ or $\beta_{k-1}(F'_i) = \beta_{k-1}(F'_i) - 1$, but not both (as can be shown via a Mayer-Vietoris sequence; see [9] and [10, pp. 120–121]).

Case 1: (β_k increases). There exists a unique birth at index i in $\mathcal{D}_k(f')$. Thus, let $j \in \bar{\mathbb{R}}$ be such that $(i, j) \in \mathcal{D}_k(f')$. Then, $(f'(\sigma_i), f'(\sigma_j)) = (i, j) \in C_B$. Define $\phi(\sigma_i) = (i, j)$.

Case 2: (β_{k-1} decreases). There is a unique death at index i in $\mathcal{D}_k(f')$. Thus, let $j \in \bar{\mathbb{R}}$ be such that $(j, i) \in \mathcal{D}_k(f')$. Then, $(f'(\sigma_j), f'(\sigma_i)) = (j, i) \in C_D$. Define $\phi(\sigma_i) = ((f'(\sigma_j), f'(\sigma_i)) = (j, i)$.

In other words, each σ_i is mapped to the persistence pair containing $f'(\sigma_i)$. If $\phi(\sigma) = \phi(\tau) = (i, j)$, then, by construction, both σ and τ are the same type of event. WLOG, assume that they are birth events. Then, $f'(\sigma) = f'(\tau)$, which, by injectivity of f' means that $\sigma = \tau$. Thus, we have shown that ϕ is an injection.

We show that ϕ is a surjection by contradiction. Suppose there exists $(i, j) \in C$ such that there does not exist $\sigma \in f^{-1}(c)$ with $\phi(\sigma) = (i, j)$. Since $(i, j) \in C$, then either $f(\sigma_i) = c$ or $f(\sigma_j) = c$ (or both). WLOG, suppose $f(\sigma_i) = c$. Then, $\sigma_i \in f^{-1}(c)$ and, by construction, $\phi(\sigma_i) = (i, j) \in C_B$.

By Equation (2) and since $\widehat{\mathcal{D}}(f)$ is well-defined (see Lemma 25), we know that $\psi: \mathcal{D}_k(f') \rightarrow \widehat{\mathcal{D}}_k(f)$ defined by $\psi(i, j) = (f(\sigma_i), f(\sigma_j))$ is a bijection. Since $C \subset \mathcal{D}_k(f')$ and both functions are bijections, the composition $\psi \circ \phi$ is the one-to-one correspondence that we sought. \square

Next, we introduce a general position assumption. Let e_i denote the i^{th} standard basis vector in \mathbb{R}^d .

Assumption 1 (General Position). *Let $V \subset \mathbb{R}^d$ be a finite set of vertices. We say V is in general position if the following properties hold:*

- (i) *Every set of $d + 1$ vertices are affinely independent.*
- (ii) *No three points are collinear in the subspace $\pi_{1,2}(\mathbb{R}^d) = \mathbb{R}^2$, where $\pi_{1,2}: \mathbb{R}^d \rightarrow \mathbb{R}^2$ is the orthogonal projection onto the plane spanned by e_1 and e_2 .*
- (iii) *All vertices have a unique height with respect to direction e_1 .*

Assumption 1(i) guarantees that, for any $V = \{v_0, v_1, \dots, v_k\} \subset K_0$, the span of $\{v_1 - v_0, v_2 - v_0, \dots, v_k - v_0\}$ is a k -dimensional affine subspace of \mathbb{R}^d , which we denote $\text{aff}(V)$. Given a simplex σ , we may use the notation $\text{aff}(\sigma)$ to mean $\text{aff}(\text{verts}(\sigma))$. Assumption 1(ii) is used in Section 3.3 to radially sort vertices and Assumption 1(iii) is used in Section 3.2 and Section 3.3; note that Assumption 1(ii) and Assumption 1(iii) are met with probability one.

To conclude this subsection, we define a structure that is used throughout the remainder of the paper to talk about lower-star filtrations in a clear way. This structure helps build a geometric intuition for several of the proofs that follow.

Definition 4 (Filtration Hyperplane). *Let $s \in \mathbb{S}^{d-1}$ be a unit vector, and let $c \in \mathbb{R}$. Let $H(s, c)$ be the $(d-1)$ -dimensional hyperplane that passes through the point $cs \in \mathbb{R}^d$ and is perpendicular to s . We define the closed half-spaces above and below this hyperplane with respect to direction s by $H^\uparrow(s, c)$ and $H^\downarrow(s, c)$, respectively.*

Let V be a finite set of vertices in \mathbb{R}^d and let $h_s: V \rightarrow \mathbb{R}$ be the lower-star filter function for direction s . The filtration hyperplanes of V are the set of hyperplanes

$$\mathbb{H}(s, V) := \{H(s, h_s(v))\}_{v \in V}.$$

All hyperplanes in $\mathbb{H}(s, V)$ are parallel to each other and perpendicular to the direction s . Let $K \in \mathbb{R}^d$ be a simplicial complex. Since the births in $\widehat{\mathcal{D}}_0(h_s)$ are in one-to-one correspondence with the vertices of K by Lemma 3, there is a filtration hyperplane at every height at which a vertex lies in direction s .

2.3 Framework for the Oracle

In this work, we show that we can reconstruct a shape from a specific set of diagrams, meaning that the directions used in the reconstruction correspond to a faithful discretization of the PHT. Because the reconstruction process begins with no knowledge of the shape, we define a framework for how these diagrams are obtained. The following definition describes an oracle that returns diagrams for a given direction and dimension.

Definition 5 (Oracle). *For a simplicial complex $K \subset \mathbb{R}^d$ and a direction $s \in \mathbb{S}^{d-1}$, the operation $\text{Oracle}(s)$ returns diagram $\widehat{\mathcal{D}}(s)$. Moreover, if a dimension $i \in \mathbb{Z}$ is specified, the oracle $\text{Oracle}_i(s)$ returns $\widehat{\mathcal{D}}_i(s)$ restricted to the i -dimensional points.¹ We define $\Theta(\Pi)$ to be the time complexity of this oracle query.*

Our primary reconstruction algorithm (Algorithm 7) discovers simplices by identifying wedges in which properties, extracted from APDs, differ. Unfortunately, one cannot form the wedges around the d -simplices in \mathbb{R}^d . As such, for the remainder of this work we assume that the highest dimensional simplex of unknown complex is $\kappa < d$. We address the case when $\kappa = d$ by describing a straightforward adaptation in Appendix C.

3 Reconstruction Algorithm for Simplicial Complexes in \mathbb{R}^n

In the following section, we describe a method for reconstructing simplicial complexes in \mathbb{R}^d . Our method first finds the locations of zero-simplices (Section 3.2), then one-simplices (Section 3.3), and then all higher-dimensional simplices (Section 3.4). We then combine these methods in our full reconstruction algorithm (Section 3.5).

We first describe a method of finding a direction that maintains certain properties. This is a fundamental tool used in various ways throughout our reconstruction algorithms.

3.1 Preliminary Construction: Finding a Tilted Direction

Given a subset of vertices $V \subset K_0$, a direction such that all vertices in V occur at unique heights, and any other direction, we can find a slight “tilt” of the first direction toward the second that maintains the order of the vertices in V . We use this tilting strategy on K_0 to reconstruct vertex locations in Section 3.2. Then, we perform tilts on smaller subsets of vertices to aid in higher-dimensional simplex reconstruction in Section 3.4.

Lemma 6 (Tilt). *Let $V \in \mathbb{R}^d$ be a set of vertices. Let $s, s' \in \mathbb{S}^{d-1}$ be linearly independent directions and let H, H' be lists of heights of vertices in s and s' respectively. Then, we can compute a third direction s_t in $\Theta(|V| \log |V| + d)$ time such that the order of vertices with respect to s_t is the same as the order of vertices with respect to s if s orders vertices in V uniquely. We refer to s_t as the tilt from s towards s' .*

¹While we can return different dimensions as separate diagrams, all persistence points computed from a given direction are computed for one diagram. In particular, we sometimes request the zeroth and first dimensions of a diagram and refer to them as separate diagrams. However, when calculating diagram complexity, we count one diagram, not two.

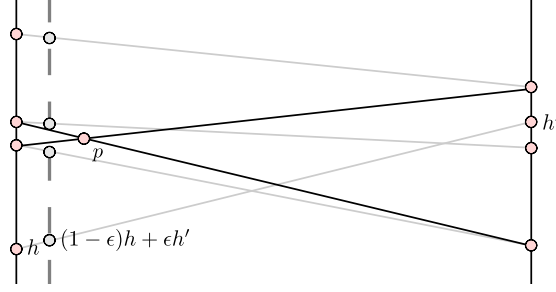


Figure 1: The light grey lines in the figure above indicate the changing heights of vertices as we swing s towards s' , where h and h' denote the heights of the indicated vertex in directions s and s' , respectively. Although these lines may be unknown in the case of vertex reconstruction, we know that no intersection of grey lines (i.e., no swapping of vertex order) occurs before the point p , which is the intersection of the closest pairwise heights of H and the extremal heights of H' , as indicated by the black lines. By choosing $\epsilon = p^{(1)}/2$, there are no crossings of line segments in S' , and thus, no change in the order of vertices with respect to direction $s_t = (1 - \epsilon)s + \epsilon s'$.

Proof. We show how to compute an ϵ so that $s_t = (1 - \epsilon)s + \epsilon s'$ is as desired. Let S be the set of line segments

$$S := \left\{ (0, h), (1, h') \right\}_{h \in H, h' \in H'},$$

Each line segment in S represents a linear interpolation between points $(0, h)$ and $(1, h')$ corresponding to the n_0^2 possible pairings of the s and s' coordinates of each $v \in V$. Moreover, we can parameterize each line segment in S as $(1 - t)h + th'$ for $t \in [0, 1]$. We want to identify a particular $\epsilon > 0$ such that the ordering of the heights of vertices in direction $s_t = (1 - \epsilon)s + \epsilon s'$ is consistent with the ordering of the vertices in direction s . To do so, let p be the left-most non-zero intersection of the line segments in S and let $p^{(1)}$ be the first coordinate of p . Then, let $\epsilon = p^{(1)}/2$. Since $\epsilon < p^{(1)}$, line segments in

$$S' := \left\{ (0, h), (\epsilon, (1 - \epsilon)h + \epsilon h') \right\}_{h \in H, h' \in H'}$$

must not have any crossings, and so the ordering of vertices is maintained. In particular, if s orders vertices uniquely, so does s_t . To find $p^{(1)}$, we note that the leftmost intersection in S is the intersection between segments connecting the closest heights in H and the extreme heights in H' ; see Figure 1.

We sort H and H' in $\Theta(|V| \log |V|)$ time. Finding p from the resulting two segments takes constant time, and returning $s_t = (1 + \epsilon)s + \epsilon s'$ takes $\Theta(d)$ time. Thus, the total runtime is $\Theta(|V| \log |V| + d)$. \square

We use tilts in higher-dimensional simplex reconstruction to retain above and below relationships, rather than explicit order of all vertices. The following corollary establishes the necessary properties.

Corollary 7. *Let $V \in \mathbb{R}^d$ be a set of vertices and $W \subseteq V$. Let $s, s' \in \mathbb{S}^{d-1}$ be orthogonal to $\text{aff}(W)$ and s_t be the tilt of s toward s' . Let $x \in V \setminus W$ and $w \in W$. Then $s \cdot w < s \cdot x$ implies $s_t \cdot w < s_t \cdot x$. Additionally, $s \cdot w = s \cdot x$ and $s' \cdot w < s' \cdot x$ implies $s_t \cdot w < s_t \cdot x$. Finally, if $s \cdot w \neq s \cdot x$ and $s_t \cdot w < s_t \cdot x$, then $s \cdot w < s \cdot x$.*

3.2 Vertex Reconstruction

Given a single zero-simplex $v \in \mathbb{R}^d$, we could use any d linearly independent vectors to identify the location of v . However, for n_0 points in \mathbb{R}^d , this approach would yield up to n_0^d possible vertex locations, requiring an additional diagram and an exhaustive search of the possible locations to decide which are true vertices in K . Belton et al. [2] takes this approach, costing $\Theta(dn_0^{d+1} + d\Pi)$ time and using $d + 1$ diagrams. Here, we offer a tradeoff: a greater number of diagrams for a lower time complexity.

The vertex reconstruction algorithm, Algorithm 2, performs a series of tilts of e_1 , ensuring that all vertices appear in the same order in each tilt. This allows us to solve for vertex locations coordinate by coordinate,

computing the heights of intersections of pairs of hyperplanes rather than checking n_0^d intersection points. Thus, our approach recovers vertex locations in sub-exponential time. In this process, we use $2d-1$ diagrams.

We first show that for any $2 \leq i \leq d$ we can find the i^{th} coordinates of all vertices, denoted $V^{(i)}$, using only two APDs specifically chosen for those coordinates.

Lemma 8 (Two-Diagram Vertex Coordinate Localization). *Let $K \subset \mathbb{R}^d$ be a simplicial complex for $d \geq 2$. Let V^i be a list of the i^{th} coordinates of all vertices. If $V^{(1)}$ is known, then we can compute $V^{(i)}$ for $i \in \{2, 3, \dots, d\}$ using two additional directional augmented persistence diagrams in time $\Theta(n_0 \log n_0 + \Pi)$.*

Proof. We prove this constructively using Algorithm 1. By Lemma 6, the vertices in direction s (chosen on Line 4) have the same order as in direction e_1 . Now, we show how we can use this ordering to compute $v^{(i)}$, the i^{th} coordinate of a vertex v . Assume that the hyperplanes in $\mathbb{H}(e_1, K_0)$ and $\mathbb{H}(s, K_0)$ are ordered by their heights in e_1 and s respectively as in Line 6 and Line 7. Suppose, without loss of generality, that v is the j^{th} vertex with respect to the e_1 direction. Then, v lies on the j^{th} hyperplane of $\mathbb{H}(e_1, K_0)$ and the j^{th} hyperplane of $\mathbb{H}(s, K_0)$, meaning that v must lie in their intersection. To compute $v^{(i)}$, we consider the equations of the two hyperplanes. Recall that the j^{th} hyperplane in $\mathbb{H}(s, K_0)$ is the set of all points $x = (x^{(1)}, x^{(2)}, \dots, x^{(d)}) \in \mathbb{R}^d$ at some height. Call this height $c_{j,s}$. Then, the j^{th} hyperplane in $\mathbb{H}(s, K_0)$ is described by the equation

$$wx^{(1)} - hx^{(i)} = c_{j,s}. \quad (4)$$

Similarly, the equation for the j^{th} hyperplane in $\mathbb{H}(e_1, K_0)$ is

$$x^{(1)} = e_1 \cdot x = c_{j,e_1}. \quad (5)$$

where c_{j,e_1} is the height of the j^{th} hyperplane in $\mathbb{H}(e_1, K_0)$. Combining Equations (4)–(5) and solving for the coordinate $x^{(i)}$, we get

$$x^{(i)} = \frac{1}{h}(wc_{j,e_1} - c_{j,s}).$$

Because v is in the intersection of these hyperplanes, its i^{th} coordinate is $\frac{1}{h}(wc_{j,e_1} - c_{j,s})$. Since j was arbitrary, the same process works for all zero-simplices in K_0 . Thus, the for loop on Line 9 computes the i^{th} coordinate of all zero-simplices and $V^{(i)}$ is returned on Line 11, as required.

Next, we consider the number of diagrams and runtime for computing coordinates. We compute two APDs, in Line 1 and Line 5, which take $\Theta(\Pi)$ time. On Line 4 we compute the tilt from e_1 to e_i . Since e_1 and e_i have only two nonzero entries, this takes $\Theta(n_0 \log n_0 + 2)$ time by Lemma 6. Line 6 and Line 7 take $\Theta(n_0 \log n_0)$ time. All other operations in Algorithm 1 take linear or constant time. Thus, we compute the i^{th} coordinate of all vertices in $\Theta(n_0 \log n_0 + d + \Pi)$ time using two APDs. \square

Algorithm 1 FindCoordinates($i, V^{(1)}, \widehat{\mathcal{D}}_0(e_1)$)

Input: $i \in \mathbb{N}$ s.t. $2 \leq i \leq d$; $V^{(1)}$, the heights of vertices in direction e_1

Output: $V^{(i)}$, the heights of vertices in direction e_i

```

1:  $\widehat{\mathcal{D}}_0(e_i) \leftarrow \text{Oracle}_0(e_i)$ 
2:  $H_1 \leftarrow V^{(1)}$ 
3:  $H_i \leftarrow \text{births in } \widehat{\mathcal{D}}_0(e_i)$ 
4:  $s \leftarrow \text{the tilt from } e_1 \text{ towards } e_i \text{ as in Lemma 6}$ 
5:  $\widehat{\mathcal{D}}_0(s) \leftarrow \text{Oracle}_0(s)$ 
6:  $H_1 \leftarrow \text{births in } \widehat{\mathcal{D}}_0(e_1) \text{ sorted in ascending order}$ 
7:  $H_s \leftarrow \text{births in } \widehat{\mathcal{D}}_0(s) \text{ sorted in ascending order}$ 
8:  $(w, -h) \leftarrow \text{the 1}^{\text{st}} \text{ and } i^{\text{th}} \text{ coordinates of } s$ 
9: for  $j \in \{1, 2, \dots, n_0\}$  do
10:    $V^{(i)}[j] \leftarrow \frac{1}{h}(wH_1[j] - H_s[j])$ 
11: return  $V^{(i)}$ 
```

Finally, Algorithm 2 reconstructs K_0 by solving for the location of all vertices coordinate by coordinate.

Algorithm 2 FindVertices()

Input: none (but makes calls to global **Oracle**)**Output:** $V = K_0$

- 1: $\widehat{\mathcal{D}}_0(e_1) \leftarrow \text{Oracle}_0(e_1)$
 - 2: $V \leftarrow$ list of n_0 d -dimensional points, with all coordinates set to null
 - 3: $V^{(1)} \leftarrow$ birth times in $\widehat{\mathcal{D}}_0(e_1)$
 - 4: **for** each i in dimensions 2 to d **do**
 - 5: $V^{(i)} \leftarrow \text{FindCoordinates}(i, V^{(1)}, \widehat{\mathcal{D}}_0(e_1))$ ▷ Algorithm 1
 - 6: **return** V
-

Theorem 9 (Reconstructing Zero-Simplices). *Let $K \subset \mathbb{R}^d$ be a simplicial complex. Then, Algorithm 2 reconstructs the vertex locations of all $v \in K_0$ using $\Theta(d)$ diagrams in $\Theta(dn_0 \log n_0 + d\Pi)$ time.*

Proof. By Lemma 8, we can find the i^{th} coordinate of vertices in K_0 with two diagrams in $\Theta(n_0 \log n_0 + \Pi)$ time, which is carried out in Algorithm 1. Algorithm 2 finds the first coordinate of vertices in K_0 and then calls Algorithm 1 to compute the vertex coordinates once for each of the $d - 1$ remaining coordinates, so Algorithm 2 uses $\Theta(d)$ diagrams and takes $\Theta(dn_0 \log n_0 + d\Pi)$ time. \square

3.3 Edge Reconstruction

Once we have identified the location of vertices we can reconstruct the edges. The algorithm that we present has runtime $\Theta(n_1 \log n_0 (n_0^2 + \Pi))$ and uses $\Theta(n_1 \log n_0)$ diagrams. In contrast, [2, Theorem 16] takes $\Theta(n_0^4 + n_0^2 \Pi)$ time and uses $n_0^2 - n_0$ diagrams. Note that for a very dense edge set, that is, when $n_1 = \Theta(n_0^2)$, the method in [2, Theorem 16] is better. But, as a single diagram tells us the number of edges, one can choose the better option based on edge density.

The main algorithm, Algorithm 4, uses a sweepline in direction e_1 , where events occur at vertices (unique by Assumption 1(iii)). We use “above (below)” as shorthand for “above (below) with respect to e_1 .” At each vertex v , we call Algorithm 3 to find all edges adjacent to and above v using a binary search for all such edges simultaneously. When each vertex is processed, the loop maintains the invariant that all edges adjacent to a vertex strictly below v are known.

To keep track of regions containing edges incident to a vertex we introduce a data structure called an *edge interval object* (Table 1). An edge interval object represents the region in the (e_1, e_2) -plane swept out between two angles α_1 and α_2 with respect to the e_2 vector and centered at a specified vertex v , and holds information about vertices and edges in this region. We make use of edge intervals only above the vertex about which they are centered, so the maximal edge interval is the upper half-plane and $\pi \leq \alpha_2 \leq \alpha_1 \leq 0$. An edge interval object stores a list of vertices sorted radially clockwise about v . By construction, the first vertex in the list must be closest to α_2 and the last closest to α_1 . The edge interval object also stores the count of edges of K_1 within the region that are adjacent to v ; observe that these edges must have vertices from **verts** as endpoints. Note that α_1 and α_2 are only used in proofs and for clarity, not by any algorithms.

Table 1: Attributes of the edge interval object.

eI	Edge Interval
v	Vertex around which interval is centered
(α_1, α_2)	Start and stop angles of the interval measured with respect to the b_2 direction
verts	List of vertices in interval radially ordered clockwise in (e_1, e_2) -plane
count	Number of edges incident to v within the interval

In order to binary search through an edge interval, we need to be able to split the interval in half. This is done in Algorithm 8. Describing the algorithm and the proof of its correctness is lengthy, so we delegate this information to Appendix B. The properties of Algorithm 8 are described in the following lemma.

Lemma 10 (Interval Splitting). *Let $K \subset \mathbb{R}^d$ be a simplicial complex, $v \in K_0$ a vertex, and \mathbf{eI} an edge interval. Then, Algorithm 8 uses two diagrams and $\Theta(n_0^2 + \Pi)$ time to split \mathbf{eI} into two new edge intervals \mathbf{eI}_ℓ and \mathbf{eI}_r with the properties:*

- (i) *The vertex sets $\mathbf{eI}_r.\text{verts}$ and $\mathbf{eI}_\ell.\text{verts}$ partition $\mathbf{eI}.\text{verts}$ into the two sets of vertices, above and below $\mathbf{eI}.v$ in direction s defined on Line 2.*
- (ii) *The new edge interval objects each contain at most half of the vertices of the original edge object.*
- (iii) *The new edge objects contain the correct edge counts; that is, $\mathbf{eI}_\ell.\text{count} = |\{v' \in \mathbf{eI}_\ell.\text{verts} \text{ s.t. } (v, v') \in K_1\}|$ and $\mathbf{eI}_r.\text{count} = |\{v' \in \mathbf{eI}_r.\text{verts} \text{ s.t. } (v, v') \in K_1\}|$.*

Assuming that all edges below a vertex v are known, Algorithm 3 finds all edges adjacent to and above v using a binary search through edge interval objects. It works by maintaining a stack of edge interval objects so that the edge interval on top is the next to be processed. If an edge interval has `count` = 0, it contains no edges, and it can be ignored (Line 6). If it has `count` = 1 and exactly one vertex, that vertex must form an edge with v and that edge is added to K_1 (Line 8). Otherwise, the edge interval is split in half using Algorithm 8, and the left interval is put on top of the right in the stack. Processing left intervals before right intervals means that we always know the edges clockwise radially preceding the intervals we try to split, a necessary condition for calling Algorithm 8. Figure 2 shows how Algorithm 8 is called multiple times during an execution of Algorithm 3 to split edge intervals until they contain a single edge.

Algorithm 3 FindUpEdges($v, E_v, V_v, \theta, \widehat{D}(s)$)

Input: $v \in K_0$; E_v , a list of edges adjacent to and below v sorted clockwise around $\pi_{1,2}(v)$; V_v , a list of vertices ordered clockwise around $\pi_{1,2}(v)$; θ , the minimum angle between distinct vertices of V_v with respect to v ; and $\widehat{D}(s)$, the APD in direction s such that s orders K_0 uniquely

Output: all edges $(v, v') \in K_1$ that are above v

- 1: $\text{Indeg} \leftarrow |(a, b) \in \widehat{D}_0(-e_1) \text{ s.t. } b = -e_1 \cdot v| + |(a, b) \in \widehat{D}_1(-e_1) \text{ s.t. } a = -e_1 \cdot v|$
 - 2: $\mathbf{eIStack} \leftarrow$ a stack of edge interval objects, initially containing a single edge interval centered at v with `count` = Indeg and `verts` the sorted array of vertices in V_v that are above v
 - 3: **while** $\mathbf{eIStack}$ is not empty **do**
 - 4: $\mathbf{eI} \leftarrow \mathbf{eIStack}.\text{pop}()$
 - 5: **if** $\mathbf{eI}.\text{count} = 0$ **then**
 - 6: Continue to top of while loop
 - 7: **if** $|\mathbf{eI}.\text{verts}| = 1$ **then**
 - 8: Append the vertex in $\mathbf{eI}.\text{verts}$ to E_v and continue to top of while loop
 - 9: $(\mathbf{eI}_\ell, \mathbf{eI}_r) \leftarrow \text{SplitInterval}(\mathbf{eI}, E_v, \theta)$ ▷ Algorithm 8
 - 10: Push \mathbf{eI}_r onto $\mathbf{eIStack}$ and then \mathbf{eI}_ℓ onto $\mathbf{eIStack}$
 - 11: **return** all edges $(v, v') \in E_v$ with $e_1 \cdot v' > e_1 \cdot v$
-

Lemma 11 (Finding Edges Above a Vertex). *Let $v \in K_0$ and E_v be a list of edges $(v, v') \in K_1$ below v , sorted clockwise around $\pi_{1,2}(v)$. Then, Algorithm 3 finds the set of edges above v using $\Theta(\deg(v) \log n_0)$ augmented persistence diagrams in $\Theta((\deg(v) \log n_0)(n_0^2 + \Pi))$ time.*

Proof. Throughout Algorithm 3 we maintain a stack $\mathbf{eIStack}$ of edge interval objects, which hold vertices and counts of edges. We think of the vertices as *potential edges* – vertices that may or may not participate in an edge with v . Let E_p be the concatenation of all vertex lists of edge intervals in $\mathbf{eIStack}$ in order.

Let V_v be a list of the vertices $K_0 \setminus v$ sorted radially clockwise around $\pi_{1,2}(v)$, beginning with the vertex with smallest angle below the horizontal in the bottom-left quadrant. By Assumption 1(ii), this ordering is well-defined. The value computed on Line 1 is the number of edges adjacent to and above v , and since s orders vertices uniquely, is correct by Lemma 3. We denote the index of a vertex v' in E_p or V_v as $E_p.\text{index}(v')$ or $V_v.\text{index}(v')$, respectively. Having defined E_p and V_v , we now give a loop invariant to prove the correctness of Algorithm 3. At the beginning of each iteration of the loop on Line 3,

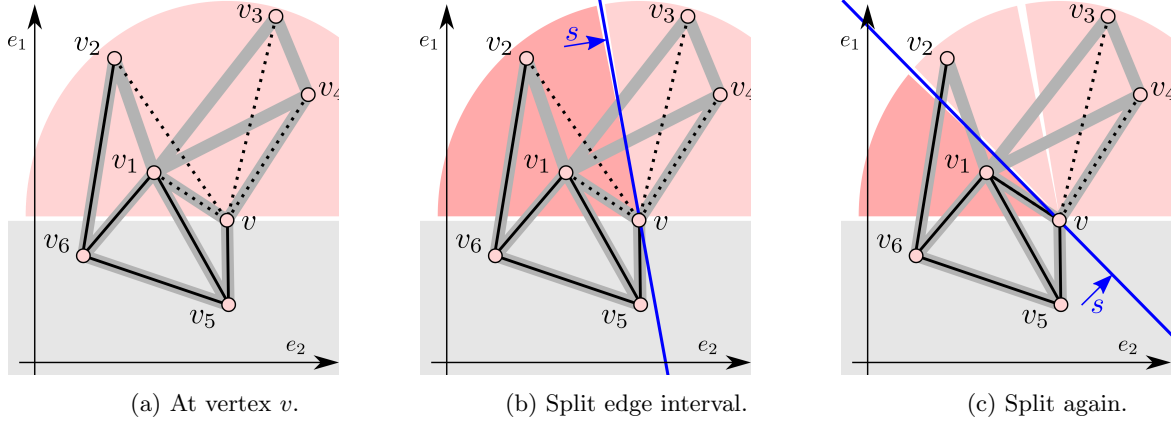


Figure 2: We demonstrate one step of Algorithm 3. (a) We initially know $[v_6, v] \in K_1$ and that two of the four vertices above v are adjacent to v , so we create an edge interval \mathbf{eI} with $\mathbf{eI.count} = 2$, and $\mathbf{eI.verts} = (v_1, v_2, v_3, v_4)$. (b) In Algorithm 8, we choose a direction s such that half of the vertices in \mathbf{eI} are below v . We use this split to create two edge intervals, \mathbf{eI}_r and \mathbf{eI}_ℓ , corresponding to the pink shaded regions on the right and left. We push \mathbf{eI}_r onto a stack to be processed later and focus on the interval \mathbf{eI}_ℓ . Since two edges contribute to v 's indegree in direction s and one is the known edge $[v_6, v]$, we have $\mathbf{eI.count} = 2 - 1 = 1$. (c) Next, we find a new direction s that splits $\mathbf{eI}_\ell.verts$ into two sets of size one. We push the set above s onto our stack. The edge interval containing only v_1 also has $\mathbf{eI.count} = 2 - 1 = 1$, so $[v_1, v] \in K_0$.

- (i) All $v' \in K_0$ adjacent to v with $V_v.index(v') < V_v.index(E_p[0])$ are in E_v (all edges to the left of the stack are known).
- (ii) If $v_1, v_2 \in E_p$ and $E_p.index(v_1) < E_p.index(v_2)$, then $V_v.index(v_1) < V_v.index(v_2)$ (the edge interval stack is clockwise-ordered).
- (iii) If $(v, v') \in K_1$, then v' is exclusively in E_v or E_p .

Assume the invariant holds entering the i^{th} iteration of the loop on Line 3. We now show that it holds entering the $(i + 1)^{\text{st}}$ iteration.

To begin the i^{th} iteration, we pop an edge interval off of $\mathbf{eIStack}$ into the variable \mathbf{eI} on Line 4. We consider three cases: the case where \mathbf{eI} contains no edges (Line 5), the case where \mathbf{eI} contains exactly one edge and exactly one vertex (Line 7), and the case where \mathbf{eI} contains at least one edge and more than two vertices (Lines 9–10).

In the first case, \mathbf{eI} contains no edges. We have removed \mathbf{eI} from $\mathbf{eIStack}$ and we do not add anything back on to $\mathbf{eIStack}$, so E_p loses the vertices from $\mathbf{eI.verts}$ but E_v does not change. Because Parts (i)–(iii) held at the beginning of the loop and we add nothing to E_v and we only remove an edge interval from $\mathbf{eIStack}$, they still hold.

In the second case, \mathbf{eI} contains exactly one edge and exactly one vertex, meaning $[\mathbf{eI.verts}[0], v] \in K_1$. We add $\mathbf{eI.verts}[0]$ to E_v in Line 8, but because \mathbf{eI} is no longer on the stack the edge $[\mathbf{eI.verts}[0], v]$ is not in E_p , and thus Part (iii) is maintained. We do not add any edge intervals back onto \mathbf{eI} , so Part (ii) is maintained as well. Finally, because Part (ii) was true at the start of the iteration, $\mathbf{eI.verts}$ was the left-most vertex in E_p . By Part (i), all edges to the left of the stack were known; adding $[\mathbf{eI.verts}[0], v]$ to E_v means that all edges left of the stack are still known, and thus Part (i) is also maintained.

In the third case, \mathbf{eI} contains at least two vertices and at least one edge. We first split \mathbf{eI} into two new edge intervals \mathbf{eI}_ℓ (left) and \mathbf{eI}_r (right) on Line 9 using Algorithm 8, and then push the right and then left back onto the stack on Line 10. By Lemma 10, vertices in \mathbf{eI}_ℓ and \mathbf{eI}_r are in sorted order, with vertices in \mathbf{eI}_ℓ coming before \mathbf{eI}_r ; thus, E_p is unchanged and Part (ii) holds. Additionally, the vertices and potential edges in the stack are unchanged, as is E_v , and so Parts (i) and (iii) hold as well.

Next, we show that when the loop ends, we return the correct answer. The loop terminates when $\mathbf{eIStack}$ is empty, which implies that E_p is also empty. Then, Part (iii) of the loop invariant implies that all vertices adjacent to v are in E_v . We then return only those vertices from E_v that are above v on Line 11, as required.

Finally, we analyze the time complexity of the algorithm and the number of diagrams it requires. The stack `eIStack` never is larger than $2 \deg(v)$ since it can only ever store one edge interval `eI` with `eI.count` = 0 for every edge interval with positive edge count. Over the course of the algorithm, we decompose the initial edge interval with edge count $O(n_0)$ into $\deg(v)$ edge intervals with exactly one vertex and one edge each. By Part (ii) of Lemma 10, each of these edge-identifying intervals makes $\Theta(\log n_0)$ calls to Algorithm 8. For any edge interval with an edge count of zero, we do nothing. Thus, the total number of calls to Algorithm 8 is $\Theta(\deg(v) \log n_0)$, and the algorithm terminates. All operations in the loop take constant time except the calls to Algorithm 8, which runs in $\Theta(n_0^2 + \Pi)$ time by Lemma 10, so the total complexity is $\Theta((\deg(v) \log n_0)(n_0^2 + \Pi))$. Furthermore, each call to Algorithm 8 requires two persistence diagrams, so the total number of persistence diagrams used is $\Theta(\deg(v) \log n_0)$. \square

Algorithm 4 FindEdges(K_0)

Input: K_0 , a list of all vertices in K

Output: K_1 , a list of all edges in K

```

1:  $\widehat{D}(-e_1) \leftarrow \text{Oracle}(-e_1)$ 
2:  $K_1 \leftarrow \{\}$ 
3: for  $v$  in  $K_0$ , in increasing height in direction  $b_1$  do
4:    $V_v \leftarrow$  vertices in  $K_0 \setminus \{v\}$ , sorted radially clockwise around  $v$ 
5:    $\theta \leftarrow$  minimum angle between any two vectors  $v_i v$  and  $v_j v$  for  $v_i \neq v_j \in V_v$ 
6:    $E_v \leftarrow v'$  for  $(v, v') \in K_1$  sorted radially clockwise around  $v$ 
7:   Add edges from FindUpEdges( $v, E_v, V_v, \theta, \widehat{D}(-e_1)$ ) to  $K_1$  ▷ Algorithm 3
8: return  $K_1$ 

```

Finally, we present the main theorem for our edge reconstruction method.

Theorem 12 (Edge Reconstruction). *Let $K \subset \mathbb{R}^d$ be a simplicial complex and $\{b_1, b_2, e_3, e_4, \dots, e_d\}$ be a basis for \mathbb{R}^d such that vertices have unique heights in direction b_1 . Given the locations of K_0 , Algorithm 4 reconstructs K_1 using $\Theta(n_1 \log n_0)$ augmented persistence diagrams in $O(n_1 \log n_0(n_0^2 + \Pi))$ time.*

Proof. In order to process vertices in order in the e_1 direction, we first sort them in Line 3. For $0 \leq j < n_0$, let v_j be the j^{th} vertex in this ordering. To show that Algorithm 4 finds all edges in K , we consider the loop invariant that when we process v_j all edges with maximum vertex height equal or less than the height of v_j are known. It is trivially true for v_0 , so we now assume that it is true for iteration j , and show that it must be true for iteration $j + 1$. By assumption, all edges (v, v_j) with v at or below v_j are known, and so by Lemma 11, Algorithm 3 finds all edges (v', v_j) where v' is strictly above v_j , and we add them to the edge set K_1 . Note that, by assumption, all edges (v, v_i) for $0 \leq i \leq j$ are also already known, and so the invariant is maintained. Thus, after the loop terminates, all edges are found.

We now analyze the runtime and diagram count for Algorithm 4. We use a single diagram in Lines 1–???. In Line 3, we sort the vertices in $\Theta(n_0 \log n_0)$ time. In Line 4, for each $v \in K_0$, we radially order the vertices of $K_0 \setminus \{v\}$ around v , and in Line 5, we find the minimum angle between vectors between v and all other vertices in K_0 . Similarly to Belton et al. [2, Theorem 14 (Edge Reconstruction)], we can find the all radial orderings and minimum angles in $\Theta(n_0^2)$ time. For each $v \in \text{simComp}_0$, we call Algorithm 3, taking $\Theta((\deg(v) \log n_0)(n_0^2 + \Pi))$ time. Summing over all vertices, we get $\Theta(n_1 \log n_0(n_0^2 + \Pi))$ time. Algorithm 3 also uses $\Theta(\deg(v) \log n_0)$ diagrams, yielding $\Theta(n_1 \log n_0)$ diagrams across all vertices. \square

3.4 Higher-Dimensional Simplex Reconstruction

In this section we give Algorithm 6, a predicate that determines whether a set of $k + 1$ zero-simplices is a k -simplex of the underlying simplicial complex. We first develop the tools needed to define Algorithm 6.

3.4.1 Computing k -Indegree

The key to determining whether a simplex exists is the k -*indegree* of a simplex, which is the count of k -dimensional cofaces of a simplex σ occurring at the same height as σ in a particular direction.

Definition 13 (*k*-Indegree for Simplex). Let $K \subset \mathbb{R}^d$ be a simplicial complex and $\sigma \in K$ be a j -simplex such that $0 \leq j < k \leq d$. Let $s \in \mathbb{S}^{d-1}$ be a direction perpendicular to $\text{aff}(\sigma)$. Then, the k -indegree of σ in direction s is the number of k -dimensional cofaces of σ that have the same height as σ in direction s .

We can compute k -indegrees by choosing directions that “isolate” a face of a simplex. We use a tilt (Corollary 7) close enough to an input direction to define a wedge of regions between filtration hyperplanes that only contains a potential k -simplex and no other vertices (see Figure 4 for an illustration of this idea). To find the tilted direction, we first find a direction toward which we will tilt.

Lemma 14 (Finding a Second Perpendicular Direction). Let $U \in \mathbb{R}^d$ be a finite set of points and $V \subseteq U$ be affinely independent with $2 < |V| \leq d$. Let $W \subseteq V$. Let $s \in \mathbb{S}^{d-1}$ be orthogonal to $\text{aff}(V)$ such that, for $v \in V$ and $u \in U \setminus V$, we have $s \cdot v \neq s \cdot u$. Then, we can find $s' \in \mathbb{S}^{d-1}$ orthogonal to $\text{aff}(W)$ such that, for all $w \in W$ and all $x \in V \setminus W$, we have $s' \cdot w < s' \cdot x$ in $\Theta(d^2)$ time.

Proof. If $W = \emptyset$, any direction trivially satisfies the conditions. If $W = V$, we choose $s = s'$. Thus, we proceed assuming $W \subsetneq V$ is nonempty. Let $p = v - s$ for some $v \in V$. Let s^* be any direction perpendicular to $\text{aff}(W \cup \{p\})$. Let $x \in V \setminus W$. Since x is not in $\text{aff}(W \cup \{p\})$, $s^* \cdot w \neq s^* \cdot x$ for all $w \in W$. If $s^* \cdot w < s^* \cdot x$, then let $s' = s^*$. Otherwise, let $s' = -s^*$. Observe that finding a direction orthogonal to $\text{aff}(W \cup \{p\})$ can be done using a single iteration of Gram-Schmidt, taking $\Theta(d^2)$ time [24]. \square

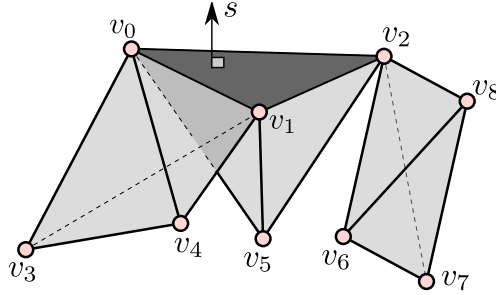


Figure 3: The three-indegree for a two-simplex (triangle) in \mathbb{R}^4 . The simplex $\sigma = [v_0, v_1, v_2]$ is shown in dark gray. The direction $s \in \mathbb{S}^2$ is normal to $\text{aff}(\sigma)$ such that all other vertices shown are below σ . The three-indegree (Definition 13) of σ is one. Using the three-indegree of all faces of σ in tilted directions, the three-indegree of σ can be defined by subtracting the indegrees of faces of σ in specific directions ($3 - 1 - 1 = 1$) given in Equation (9). The APD in direction s sees three tetrahedron at the same height as σ , which is why we need the recursive definition.

Although choosing s orthogonal to $\text{aff}(\sigma)$ means all zero-simplices of σ are at the same height in direction s , not all k -simplices at this height contribute to the k -indegree of σ as shown in Figure 3. Thus, we use the direction computed in Lemma 14 to find a tilted direction s_t , which, together with s can be used to compute k -indegree. The algorithm for doing so (Algorithm 5) is given below. To prove its correctness, we make the following observation.

Lemma 15 (Unique Face Isolation). Let $j < k \leq d \in \mathbb{N}$. Let $K \subset \mathbb{R}^d$ be a simplicial complex. Let τ be a j -simplex with $\tau \prec \sigma \in K$. Let $s \in \mathbb{S}^{d-1}$ be orthogonal to $\text{aff}(\sigma)$ such that for all $v \in \sigma$ and $u \in K_0 \setminus \text{verts}(\sigma)$, $s \cdot v \neq s \cdot u$, let $s' \in \mathbb{S}^{d-1}$ be orthogonal to $\text{aff}(\sigma)$ so that $\text{verts}(\sigma \setminus \tau)$ are above $\text{verts}(\tau)$ with respect to s' as in Lemma 14, and let $s_t \in \mathbb{S}^{d-1}$ be the tilt of s toward s' as in Corollary 7. Let $\sigma' \in K$ be a k -simplex at the same height as σ in direction s_t . Then, σ' contributes to the k -indegree of τ in direction s_t if and only if $\tau = \sigma \cap \sigma'$.

Proof. Let $f: K \rightarrow \mathbb{R}$ ($f_t: K \rightarrow \mathbb{R}$, respectively) be the filter function for direction s (s_t , respectively).

(\Rightarrow) Suppose that σ' contributes to the k -indegree of τ in direction s_t . Then, by the definition of k -indegree, $\tau \prec \sigma'$. Since $\tau \prec \sigma$ by assumption, we have $\tau \preceq \sigma \cap \sigma'$. We must now show that $\sigma \cap \sigma' \preceq \tau$.

By contradiction, suppose that $\sigma \cap \sigma' \not\preceq \tau$. Then, there exists a vertex $v \in \sigma \cap \sigma'$ such that $v \notin \tau$. However, $v \in \sigma \cap \sigma'$, $v \in \sigma \setminus \text{verts}(\tau)$. Therefore, $s_t \cdot v > s_t \cdot w$ for all $w \in \text{verts}(\tau)$ by Corollary 7, a

Algorithm 5 $\text{ComputeIndegree}(\sigma, s, k, T = \{\})$

Input: $\sigma \in K$; $s \in \mathbb{S}^{d-1}$ such that $\exists c \in \mathbb{R}$ where $v \cdot s = c$ for all $v \in \sigma$ and $u \cdot s \neq c$ for all $v \in K_0 \setminus \text{verts}(\sigma)$; $k \in \mathbb{N}$ s.t. $k > \dim(\sigma)$; and table T for memoization

Output: the k -indegree for σ

```

1:  $\widehat{\mathcal{D}}_{k-1}(s), \widehat{\mathcal{D}}_k(s) \leftarrow (k-1)^{\text{st}}$  and  $k^{\text{th}}$  APDs from  $\text{Oracle}_{k-1}(s)$  and  $\text{Oracle}_k(s)$ 
2:  $c \leftarrow$  height of  $\sigma$  in direction  $s$ 
3:  $\text{numDeaths} \leftarrow$  number of deaths in  $\widehat{\mathcal{D}}_{k-1}(s)$  at height  $c$ 
4:  $\text{numBirths} \leftarrow$  number of births in  $\widehat{\mathcal{D}}_k(s)$  at height  $c$ 
5:  $\text{doubleCounts} \leftarrow 0$ 
6: for  $\tau \prec \sigma$  in non-descending order by dimension do
7:   if  $T[\tau]$  was not computed yet then
8:      $s' \leftarrow$  direction orthogonal to  $\text{aff}(\tau)$  so that  $\text{verts}(\sigma \setminus \tau)$  are above  $\text{verts}(\tau)$ , as in Lemma 14
9:      $s_t \leftarrow$  the tilt of  $s$  toward  $s'$  as in Corollary 7
10:     $T[\tau] \leftarrow \text{ComputeIndegree}(\tau, s_t, k, T)$ 
11:     $\text{doubleCounts} \leftarrow \text{doubleCounts} + T[\tau]$ 
12: return  $\text{numDeaths} + \text{numBirths} - \text{doubleCounts}$ 

```

contradiction to the claim that σ' contributes to the k -indegree of τ in direction s_t . Therefore, $\sigma \cap \sigma' \preceq \tau$ as required.

(\Leftarrow) Suppose that $\tau = \sigma \cap \sigma'$. Since σ' is a k -simplex, τ is a j -simplex, and $\tau \prec \sigma'$, we can write $\tau = [v_0, v_1, \dots, v_j]$ and $\sigma' = [v_0, v_1, \dots, v_k]$ where $v_i \in K_0$. Then,

$$f_t(\sigma') = \max_{i=0}^k f_t(v_i) = \max \left(\max_{i=0}^j f_t(v_i), \max_{i=j+1}^k f_t(v_i) \right) = \max \left(f_t(\tau), \max_{i=j+1}^k f_t(v_i) \right). \quad (6)$$

Since σ' is at the same height as σ in direction s_t and $\tau \prec \sigma$, σ' is also at the same height as τ in direction s , meaning that $f(v_i) \leq f(\tau)$ for all $0 \leq i \leq k$. Since v_i is not in τ for $i > j$, it must also be the case that $f(v_i) < f(\tau)$ for $i > j$. By Corollary 7, any vertex below τ in direction s is also below τ in direction s_t . Thus, $f_t(v_i) < f_t(\tau)$ for all $j < i \leq k$ and

$$\left(\max_{i=j+1}^k f_t(v_i) \right) < f_t(\tau).$$

Then, by Equation (6), $f_t(\sigma') = f_t(\tau)$. This taken together with $\tau \prec \sigma'$ shows that σ' contributes to the k -indegree of τ in direction s_t . \square

Since Lemma 15 shows that a single diagram is not sufficient to compute the k -indegree, we use an inclusion-exclusion style argument to compute the k -indegree in Algorithm 5. The first time this algorithm is called, we have not yet computed any entries of T . Additionally, note that the algorithm is well-defined for $k = 1$, and the computation in Line 12 is exactly what is computed in Algorithm 3, Line 1. We prove the correctness of Algorithm 5 in the following theorem.

Theorem 16 (Computing k -indegree). *Let $K \subset \mathbb{R}^d$ be a simplicial complex. Let $\sigma \in K$. Let $s \in \mathbb{S}^{d-1}$ be a direction that is perpendicular to σ , but not to any other subset of vertices in K_0 . For $k > \dim(\sigma)$, $\text{ComputeIndegree}(\sigma, s, k)$ returns the k -indegree of σ in direction s .*

Proof. We prove the claim inductively on $j = \dim(K)$. For the base case ($j = 0$), let $k > j$ and consider the zero-simplex $[v]$. We note that this base case is a generalization of [2, Lemma 11]. Let $f_1: K \rightarrow \mathbb{R}$ be the filter function for direction s_1 . We note that, unlike in [2, Lemma 11], we are only making an argument for the k -indegree at a single vertex and not all vertices. As such, we can relax the requirement that no two vertices in K_0 have the same height in direction s and just require that no vertices in $K_0 \setminus \{v\}$ have the same height in direction s as v . Thus, we have that k -indegree of σ is equal to the number of k -simplices that have height $f(v)$, which, by Lemma 3, is:

$$|f^{-1}(f(v))| = \left| \{(a, b) \in \widehat{\mathcal{D}}_{k-1}(s) \text{ s.t. } b = f(v)\} \right| + \left| \{(a, b) \in \widehat{\mathcal{D}}_k(s) \text{ s.t. } a = f(v)\} \right|. \quad (7)$$

In Algorithm 5, notice that if σ is a single vertex, we do not enter the loop that starts on Line 6. Thus, the return value is exactly the number given in Equation (7).

For the inductive assumption, let $j \geq 0$. We assume that Algorithm 5 returns the k' -indegree of τ in direction s , for all $\tau \in K_j$ and all $k' > j$.

For the inductive step, let $\sigma \in K_{j+1}$. Let $k > j + 1$. Now, we compute the k -indegree of σ in direction s . Using Lemma 3, we know that the number of k -simplices with height $f(\sigma)$ in direction s is:

$$\delta := \left| \{(a, b) \in \widehat{\mathcal{D}}_{k-1}(s) \text{ s.t. } b = f(\sigma)\} \right| + \left| \{(a, b) \in \widehat{\mathcal{D}}_k(s) \text{ s.t. } a = f(\sigma)\} \right|. \quad (8)$$

Let F_σ denote this set of simplices, let $\sigma' \in F_\sigma$, and let $\tau \prec \sigma$. Let s' be orthogonal to $\text{aff}(\tau)$ so that $\text{verts}(\sigma \setminus \tau)$ are above $\text{verts}(\tau)$ as in Lemma 14 and s_t be the tilt of s toward s' as in Corollary 7. By Lemma 15, the k -simplex σ' contributes to the k -indegree of τ in direction s_t if and only if $\tau = \sigma \cap \sigma'$.

Then, we can isolate each face of $\tau \prec \sigma$ and compute the k -indegree of τ using Equation (8) and add or subtract it from the k -indegree of σ , alternating by dimension of τ . This ensures that no coface of $\tau \prec \sigma$ will add to the k -indegree of σ . Formally, this is seen in the equation for the k -indegree of σ

$$\delta - \sum_{\tau \prec \sigma} \delta_\tau, \quad (9)$$

where δ_τ is the k -indegree of τ in the corresponding tilted directions. In Algorithm 5, `numDeaths+numBirths` is equal to δ , and the values δ_τ are computed in Line 10 of Algorithm 5. Thus, the return value matches Equation (9). \square

Finally, the runtime of Algorithm 5 is given below.

Theorem 17 (Algorithm 5 Complexity Bounds). *Let $K \subset \mathbb{R}^d$ be a simplicial complex. Let $\sigma \in K_i$ and let $v \in \text{verts}(\sigma)$. Let $s \in \mathbb{S}^{d-1}$ be a direction perpendicular to $\text{aff}(\sigma)$ such that for all $u \in K_0$, $s \cdot u = s \cdot v$ if and only if $u \in \text{verts}(\sigma)$. Then, we have the following time complexities for Algorithm 5.*

- (i) *If $\sigma \in K_0$, then `ComputeIndegree`($\sigma, s, 1$) uses one diagram and runs in $\Theta(n_0^2 + \Pi)$ time.*
- (ii) *Otherwise, if $\sigma \in K_i$ for $i > 0$, then `ComputeIndegree`(σ, s, k) uses $2^{i+1} - 1$ diagrams and runs in $O(2^{i+1}(n_0(n_{k-1} + \log n_0) + d^2 + 2^i + \Pi))$ time.*

Proof. If $i = 0$ and $k = 1$, then we prove Part (i). The loop is never entered and we compute one diagram in time $\Theta(\Pi)$ and count $\Theta(n_0^2)$ points in the diagram.

To prove Part (ii), we focus our attention on the for loop that begins on Line 6. In this loop, we iterate through the proper faces of σ . The i -simplex σ has $2^{i+1} - 2$ faces so the loop iterates $2^{i+1} - 2$ times. However, when processing a new simplex $\tau \prec \sigma$ for the first time, we need to create the table entry $T[\tau]$. To compute the entry, we find a new direction s_t so that all vertices of $\sigma \setminus \tau$ are above τ in direction s_t and only vertices of τ share τ 's height in direction s_t on Line 9. We then recursively call Algorithm 5 on Line 10. Since faces of σ are processed in non-descending order, by the time we process τ , all of the faces of τ (which are also faces of σ and have dimension less than $\dim(\tau)$) have table entries. As a result, the recursive calls never go more than one level deep. Since recursive calls are only made when iterating through the faces of σ , there are $O(2^{i+1})$ calls made on Line 10. Each call gets the k^{th} and $(k-1)^{\text{st}}$ diagrams on Line 1 and counts the births and deaths on Lines 3–4 taking $O(n_{k-1}n_0 + \Pi)$ time. Then, since $\tau \prec \sigma$, we iterate through the $O(2^i)$ faces of τ , never entering the conditional on Line 7, to sum up the entries from T in time $O(2^i)$. Moreover, to make each recursive call, we also compute s' in $\Theta(d^2)$ time on Line 8 and a tilted direction s_t in $\Theta(n_0 \log n_0 + d)$ time on Line 9. Summing these values, we find the total runtime of Algorithm 5 for an i -simplex is $O(2^{i+1}(n_0(n_{k-1} + \log n_0) + d^2 + 2^i + \Pi))$.

Finally, we consider the number of diagrams used by Algorithm 5. Observe that we use one diagram for each call to Algorithm 5. As we recursively call this function on each face of σ , we use $2^{i+1} - 1$ APDs. \square

3.4.2 Simplex Predicate

Using the k -indegree, we are able to isolate potential k -simplices between two hyperplanes centered at a simplex. We call this double-cone shaped region a *wedge*; see Figure 4. Wedges generalize the “bow tie” used for identifying edges in [1].

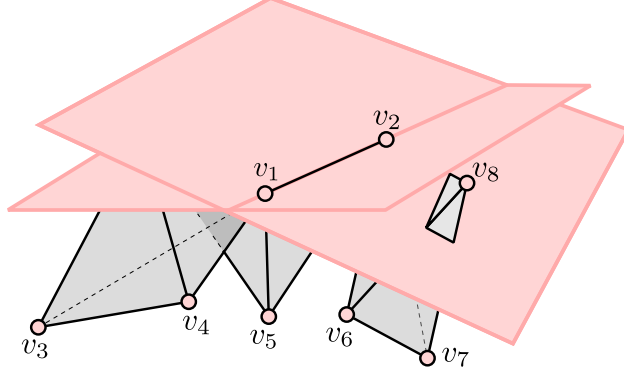


Figure 4: A wedge (shaded in pink) centered at the one-simplex $[v_1, v_2]$ that isolates vertices v_1, v_2 , and v_8 . To test if $[v_1, v_2, v_8]$ forms a two-simplex, we notice that the two-indegrees for $[v_1, v_2]$ in the two directions defining the wedge do not differ, indicating that v_1, v_2 , and v_3 do not define a two-simplex in K by Theorem 19.

Definition 18 (Wedge). *Let $P \subset \mathbb{R}^d$ be a set of points such that $|P| < \infty$ and $\text{aff}(P) \neq \mathbb{R}^d$. Let $s_1, s_2 \in \mathbb{S}^{d-1}$ be orthogonal to $\text{aff}(P)$. Let h_1, h_2 be the height of P with respect to s_1 and s_2 , respectively. The wedge between s_1 and s_2 at P is the closure of the symmetric difference between $H^\downarrow(s_1, h_1)$ and $H^\downarrow(s_2, h_2)$, which we denote as $H^\downarrow(s_1, h_1) \triangle H^\downarrow(s_2, h_2)$.*

In Algorithm 6, we use the difference in the indegree between the two filtration hyperplanes defining a wedge to test for the presence of a $(k+1)$ -simplex.

Algorithm 6 $\text{IsSimplex}(\sigma, v)$

Input: $\sigma \in K_{k-1}$ and $v \in K_0 \setminus \text{verts}(\sigma)$

Output: **True** if $\sigma \cup \{v\} \in K_k$, **False** otherwise

- 1: $k \leftarrow \text{dimension of } \sigma + 1$
 - 2: $s_1 \leftarrow \text{direction orthogonal to } \text{aff}(\text{verts}(\sigma) \cup \{v\})$
 - 3: $s_2 \leftarrow \text{direction orthogonal to } \text{aff}(\text{verts}(\sigma) \cup \{v\})$ so that no vertices of $K_0 \setminus (\text{verts}(\sigma) \cup \{v\})$ are at the same height as vertices of $\text{verts}(\sigma) \cup \{v\}$ (see Lemma 14)
 - 4: $H_1, H_2 \leftarrow$ lists of the heights of all vertices in directions s_1 and s_2 , respectively
 - 5: $s_* \leftarrow$ the tilt of s_1 toward s_2
 - 6: $s_3 \leftarrow \text{direction orthogonal to } \text{aff}(\text{verts}(\sigma))$ so that v is above vertices of $\text{verts}(\sigma) \cup \{v\}$ (see Lemma 14)
 - 7: $H_*, H_3 \leftarrow$ lists of the heights of all vertices in directions s_* and s_3 , respectively
 - 8: $s_L \leftarrow$ the tilt of s_* toward s_3
 - 9: $s_U \leftarrow$ the negative of the direction returned by tilting $-s_*$ toward $-s_3$
 - 10: **return** $|\text{ComputeIndegree}(\sigma, s_U, k) - \text{ComputeIndegree}(\sigma, s_L, k)| = 1 \triangleright \text{Algorithm 5}$
-

Theorem 19 (Correctness of Simplex Predicate). *Let $K \subset \mathbb{R}^d$ be a simplicial complex. Let $k \in \mathbb{N}$, $\sigma \in K_{k-1}$, and $v \in K_0 \setminus \text{verts}(\sigma)$. Then, Algorithm 6 returns **True** iff $\text{verts}(\sigma) \cup \{v\}$ defines a k -simplex in K in time $O(2^k(n_0(n_{k-1} + \log n_0) + d^2 + 2^{k-1} + \Pi) + dn_0)$ with $2^{k+1} - 2$ diagrams.*

Proof. Let $\Sigma = \text{verts}(\sigma) \cup \{v\}$. We are testing if Σ defines a k -simplex in K . In what follows, let $q \in K_0 \setminus (\text{verts}(\Sigma))$, $u \in \text{verts}(\Sigma)$, and $w \in \text{verts}(\sigma)$ be any vertices in their respective vertex sets. First, we compute initial direction s_1 that is orthogonal to $\text{aff}(\Sigma)$ using a single iteration of Gram-Schmidt in $\Theta(d^2)$ time [24]. However, s_1 may be orthogonal to the affine space spanned by additional zero-simplices not just in Σ , so we next find a direction s_2 orthogonal to $\text{aff}(\text{verts}(\sigma) \cup \{v\})$, but so $s_2 \cdot u \neq s_2 \cdot q$, which is possible in $\Theta(d^2)$ time by Lemma 14. This then means that s_* , the tilt of s_1 towards s_2 has the property that $s_* \cdot u \neq s_* \cdot q$ by Corollary 7. Next, we find s_3 perpendicular to $\text{aff}(\sigma)$ but not $\text{aff}(\Sigma)$, as in Lemma 14. Namely, we have $s_3 \cdot u < s_3 \cdot w$ and $s_3 \cdot u \neq s_3 \cdot q$.

Finally, we find the directions that define the upper and lower hyperplanes of the wedge (denoted s_L and s_U , respectively). Note that all vertices of σ are at the same height with respect to s_L and s_U , and we denote these heights by c_U and c_L , respectively.

To prove the correctness of Algorithm 6, we first show that $v \in \mathbb{W} := H^\downarrow(s_L, c_L) \triangle H^\downarrow(s_U, c_U)$. Since $s_* \cdot w = s_* \cdot v$ and $s_3 \cdot w < s_3 \cdot v$, we have $c_L = s_L \cdot w < s_L \cdot v$ by Corollary 7. By similar reasoning, we see that $c_U > s_U \cdot v$. Thus, $v \notin H^\downarrow(s_L, c_L)$ and $v \in H^\downarrow(s_U, c_U)$, which means that $v \in \mathbb{W} := H^\downarrow(s_L, c_L) \triangle H^\downarrow(s_U, c_U)$.

Next, we show that v is the only vertex in $(K_0 \setminus \text{verts}(\sigma)) \cap \mathbb{W}$. Assume, for contradiction, that there exists a vertex $v' \in \mathbb{W} \cap K_0 \setminus \Sigma$. Then, $c_L < s_L \cdot v'$ and since additionally $s_* \cdot w \neq s_* \cdot v'$, we have, $s_* \cdot w < s_* \cdot v'$ by Corollary 7. Furthermore, $s_U \cdot v' < c_U$, which, again by Corollary 7, implies that $-s_* \cdot v' < -s_* \cdot w$, meaning that $s_* \cdot v' < s_* \cdot w$ for all $w \in \text{verts}(\sigma)$, a contradiction. Thus, v is the only vertex in \mathbb{W} , as required.

We now show that the k -indegree can be used to determine if Σ defines a simplex in K . Recall that every k -dimensional coface of σ must contain all of the vertices of σ , plus exactly one more. Since $v \notin H^\downarrow(s_L, c_L)$ and $v \in H^\downarrow(s_U, c_U)$, every simplex that contributes to the k -indegree of σ in direction s_U also contributes to the k -indegree of σ in direction s_L . In addition, the only potential simplex contributing to the k -indegree of σ in direction s_U that does not contribute to the k -indegree in direction s_L is the one defined by $\text{verts}(\sigma)$ and v . Thus, Algorithm 6 returns **True** iff Σ defines a k -simplex.

We compute s_1 orthogonal to $\text{aff}(\Sigma)$ on Line 2 using a single iteration of Gram-Schmidt in $\Theta(d^2)$ time [24]. Computing directions s_2 and s_3 (Lines 2 and 6 also takes $\Theta(d^2)$ time by Lemma 14. We compute lists of vertex heights on Lines 4 and 7, each list costing $\Theta(dn_0)$ time. We use these lists to compute three tilted directions, each costing $\Theta(n_0 \log n_0 + d)$ time and zero diagrams by Lemma 6. Finally, we use Algorithm 5 to compute the k -indegree from two directions, taking time $O(2^{i+1}(n_0(n_{k-1} + \log n_0) + d^2 + 2^i + \Pi))$ and $2^{i+1} - 1$ diagrams by Theorem 17. Because $i = k - 1$, our complexity is $O(2^k(n_0(n_{k-1} + \log n_0) + d^2 + 2^{k-1} + \Pi) + dn_0)$ time. No diagrams are computed until we calculate k -indeg and thus, we compute $2(2^k - 1) = 2^{k+1} - 2$ diagrams. \square

Remark 20 (Forget the Heights). *While our oracle gives us the persistence diagrams for each queried direction, we do not use all of the information in the persistence diagram. In fact, if the vertex locations are known, then we are only using the total order of the vertices (with respect to the query direction) in the algorithms in this subsection. Specifically, for each direction s and each vertex $v \in K_0$, we define an equivalence relation on K such that the equivalence class for v is: $[v]_s := \{\sigma \in K \text{ s.t. } h_s(\sigma) = h_s(v)\}$. The set of equivalence classes is totally ordered by the height in direction s . Thus, in Algorithm 5 (and hence Algorithm 6), we only use the count of the number of k -simplices in each equivalence class.*

3.5 Putting It All Together: Simplicial Complex Reconstruction

Combining the results from the previous subsections, we arrive at Algorithm 7 that fully reconstructs an embedded simplicial complex. We explicitly reconstruct the edges using the technique in Section 3.3 due to the output sensitive time complexity.

Algorithm 7 ReconstructComplex()

Input: none (but makes calls to global **Oracle**)

Output: simplicial complex K

```

1:  $K_0 \leftarrow \text{FindVertices}()$  ▷ Algorithm 2
2:  $K_1 \leftarrow \text{FindEdges}(K_0)$  ▷ Algorithm 4
3: for  $i \in \{2, 3, \dots, \kappa\}$  do
4:   for  $\sigma \in K_{i-1}$  do
5:     for  $v \in K_0 \setminus \text{verts}(\sigma)$  do
6:       if  $\text{IsSimplex}(\sigma, v)$  then
7:         Add  $\sigma \cup \{v\}$  to  $K_i$ 
8: return  $K_0 \cup K_1 \cup \dots \cup K_\kappa$ 
```

Theorem 21 (Simplicial Complex Reconstruction). *Let K be a simplicial complex in \mathbb{R}^d with dimension $\kappa < d$. If K meets Assumption 1 (General Position), then Algorithm 7 reconstructs K in $O(2^\kappa nn_0(nn_0 + d^2 + 2^\kappa + \Pi) + dnn_0^2 + d\Pi)$ time using $O(nn_0 2^\kappa + d)$ diagrams.*

Proof. First, Algorithm 7 finds all vertices by making a call to Algorithm 2, whose correctness is shown in Theorem 9. Next, Algorithm 7 finds all edges by making a call to Algorithm 4, whose correctness is shown in Theorem 12. Algorithm 7 then iterates through each $(k-1)$ -simplex σ and checks whether σ forms a k -simplex with each v (for $1 < k < d$). By Theorem 19, Algorithm 6 ($\text{IsSimplex}(\sigma, v)$) determines if the simplex defined by σ and v is present in K . Since we pass every potential k -simplex to $\text{IsSimplex}(\sigma, v)$, the algorithm finds all k -simplices.

Next, we analyze the runtime. We begin by analyzing the nested loops that identify higher-dimensional simplices. The first loop on Lines 3–7 performs at most κ iterations. The second loop on Lines 4–7 performs at most n_{i-1} iterations. The third loop on Lines 5–7 performs at most n_0 iterations. Inside the inner loop, Line 6 calls $\text{IsSimplex}(\sigma, v)$, which for dimension k , takes $O(2^k(n_0(n_{k-1} + \log n_0) + d^2 + 2^{k-1} + \Pi) + dn_0)$ time by Theorem 19. Thus, after rewriting, the time is proportional to

$$\sum_{k=2}^{\kappa} n_{k-1} n_0 \left(\underbrace{dn_0}_{(10)} + 2^k \left(\underbrace{n_0 n_{k-1}}_{(11)} + \underbrace{n_0 \log n_0}_{(12)} + \underbrace{d^2}_{(13)} + \underbrace{2^{k-1}}_{(14)} + \underbrace{\Pi}_{(15)} \right) \right)$$

We can bound the running time of the loops by expanding the polynomial and bounding each monomial:

$$\sum_{k=2}^{\kappa} n_{k-1} n_0^2 d = dn_0^2 \sum_{k=2}^{\kappa} n_{k-1} \leq dnn_0^2 \quad (10)$$

$$\sum_{k=2}^{\kappa} n_{k-1} n_0 2^k (n_0 n_{k-1}) = n_0^2 \sum_{k=2}^{\kappa} 2^k n_{k-1}^2 \leq 2^{\kappa} n_0^2 \sum_{k=2}^{\kappa} n_{k-1}^2 \leq 2^{\kappa} n^2 n_0^2 \quad (11)$$

$$\sum_{k=2}^{\kappa} n_{k-1} n_0 2^k (n_0 \log n_0) = n_0^2 \log n_0 \sum_{k=2}^{\kappa} n_{k-1} 2^k \leq 2^{\kappa} n_0^2 \log n_0 \sum_{k=2}^{\kappa} n_{k-1} \leq 2^{\kappa} n n_0^2 \log n_0 \quad (12)$$

$$\sum_{k=2}^{\kappa} n_{k-1} n_0 2^k (d^2) = d^2 n_0 \sum_{k=2}^{\kappa} 2^k n_{k-1} \leq 2^{\kappa} d^2 n_0 \sum_{k=2}^{\kappa} n_{k-1} \leq 2^{\kappa} d^2 n n_0 \quad (13)$$

$$\sum_{k=2}^{\kappa} n_{k-1} n_0 2^k (2^{k-1}) = n_0 \sum_{k=2}^{\kappa} 2^{2k-1} n_{k-1} \leq 2^{2\kappa} n_0 \sum_{k=2}^{\kappa} n_{k-1} \leq 2^{2\kappa} n n_0 \quad (14)$$

$$\sum_{k=2}^{\kappa} n_{k-1} n_0 2^k (\Pi) = n_0 \Pi \sum_{k=2}^{\kappa} 2^k n_{k-1} \leq 2^{\kappa} n_0 \Pi \sum_{k=2}^{\kappa} n_{k-1} \leq 2^{\kappa} n n_0 \Pi. \quad (15)$$

Rewriting and simplifying, we get

$$\sum_{k=2}^{\kappa} n_{k-1} n_0 (dn_0 + 2^k (n_0 n_{k-1} + n_0 \log n_0 + d^2 + 2^{k-1} + \Pi)) \leq 2^{\kappa} n n_0 (n n_0 + d^2 + 2^{\kappa} + \Pi) + d n n_0^2$$

Next, we consider Line 1, in which we find the vertices in $\Theta(dn_0 \log n_0 + d\Pi)$ time. Monomials $dn_0 \log n_0$ and $d^2 n_0$ are dominated the bound in Equation (11); $d\Pi$, however, is not dominated. In Line 2, we find the edges in $\Theta(n_1 \log n_0 (n_0^2 + \Pi))$. Expanding, we get $n_0^2 n_1 \log n_0$, which is dominated by the bound in Equation (12), and $\Pi n_1 \log n_0$ is dominated by the bound in Equation (15). Finally, as $n_0 \log n_0 = O(n n_0)$, we get that the algorithm takes $O(2^{\kappa} n n_0 (n n_0 + d^2 + 2^{\kappa} + \Pi) + d n n_0^2 + d\Pi)$ time.

Next, we count the number of diagrams. Again, we begin by analyzing the nested loops that identify higher-dimensional simplices. Recall that by Theorem 19, for dimension k , $\text{IsSimplex}(\sigma, v)$ uses $2^{k+1} - 2$ diagrams. Similar to the analysis above,

$$\sum_{k=2}^{\kappa} n_{k-1} n_0 (2^{k+1} - 2) \leq n_0 \sum_{k=2}^{\kappa} n_{k-1} 2^{k+1} \leq 2 n_0 2^{\kappa} \sum_{k=2}^{\kappa} n_{k-1} \leq 2 n n_0 2^{\kappa} \quad (16)$$

We find the vertices and edges using $\Theta(d)$ and $\Theta(n_1 \log n_0)$ diagrams, respectively. The number of diagrams from finding edges is dominated by Equation (16). Thus, the algorithm uses $O(n n_0 2^{\kappa} + d)$ diagrams. \square

Recall from Section 2.3 that if the complex contains codimension-zero simplices, that is, $\kappa = d$, it is necessary to use a modified oracle that returns APDs for a parabolic lift of K . Further discussion for this case can be found in Appendix C.

Finally, we observe that through our reconstruction algorithm, we have an explicit discretizations of the PHT and other dimension-returning transforms.

Corollary 22 (A Discretization of the PHT). *Let K be a simplicial complex in \mathbb{R}^d with dimension $\kappa < d$. If K meets Assumption 1 (General Position), then the $O(nn_0 2^\kappa + d)$ APDs found in Algorithm 7 correspond to a discretization of the PHT of K .*

Since our algorithm only requires knowledge of the height and parity of each simplex in a given direction, our results can be extended to any topological descriptor that contains this information, which we call *dimension-returning transforms*, including the BCT.

Corollary 23 (A Discretization of the BCT and Other Dimension Returning Transforms). *Let K be a simplicial complex in \mathbb{R}^d with dimension $\kappa < d$. If K meets Assumption 1 (General Position), then the $O(nn_0 2^\kappa + d)$ directions used in Algorithm 7 correspond to a discretization of the BCT and other dimension-returning transforms for K .*

We can reconstruct embedded graphs using $\Theta(n_1 \log n_0 + d)$ descriptors. By observing that in \mathbb{R}^2 , $n_1 = O(n_0)$, we get discretizations of the PHT, BCT, and other dimension-returning transforms whose sizes are subquadratic.

Corollary 24 (Discretization of Transforms for Graphs Embedded in \mathbb{R}^2). *Let G be an embedded graph in \mathbb{R}^2 with n_0 vertices. If G meets Assumption 1 (General Position), then the APDs found in Algorithm 7 correspond to a size $\Theta(n_0 \log n_0)$ discretization of the PHT, BCT, and other dimension-returning transforms of G .*

4 Discussion

Here, we provide a brief discussion of how to adapt our reconstruction algorithm to topological transforms that are not dimension-returning, namely, the Euler Characteristic Curve Transform. We then conclude with a summary of our results and a survey of ongoing work.

Extension to ECCT and Other Topological Transforms Unlike the PHT or BCT, the Euler Characteristic Curve Transform (ECCT) is not a dimension-returning transform. AECCs only return the heights of simplices and a count of even and odd simplices of the sublevel set below the simplex (see Appendix A.3 for a more detailed definition of the AECC). In this section, we briefly discuss how our methods can be adapted to show discretizations of other topological transforms such as the ECCT.

Since the vertex reconstruction algorithms of section Section 3.2 rely on the presence of events rather than their dimension, our vertex reconstruction method can be directly adapted for AECCs. However, the edge reconstruction algorithms of Section 3.3 and Section 3.4 will fail for a transform that is not dimension-returning, since `ComputeIndegree` relies on knowing k -dimensional deaths and $(k-1)$ -dimensional births. We explain next how to adapt the methods of Section 3.4 to reconstruct higher-dimensional simplices (including edges) using the AECC.

Recall that the higher-dimensional simplex reconstruction algorithms (in particular, `IsSimplex`, Algorithm 6) operate by forming wedges centered at $(k-1)$ -simplices that contain only one other vertex. We can determine if the union of the $(k-1)$ -simplex and the vertex form a k -simplex using an inclusion-exclusion principle. If we are instead using AECCs, the inclusion-exclusion principle under the hood of Algorithm 6 translates to checking whether the count of even or odd simplices increases or remains the same (when k is even or odd). In particular, Line 10 of Algorithm 6 would be adapted to be the difference of Euler characteristics in s_1 and s_2 . Taken together, this means that we can define a reconstruction algorithm when our tool of reconstruction is the AECC, meaning that we have found an explicit faithful discretization of the ECCT.

Conclusion We provide a deterministic algorithm for computing the complete reconstruction of a simplicial complex embedded in arbitrary finite dimension using $O(nn_02^\kappa + d)$ APDs and $O(2^\kappa nn_0(nn_0 + d^2 + 2^\kappa + \Pi) + dnn_0^2 + d\Pi)$ time where n is the total number of simplices, n_0 is the number of vertices and κ is the dimension of the highest dimensional simplex. This algorithm also improves on the results of [1,2] for the case of plane and embedded graphs. This reconstruction algorithm serves as a proof that the resulting discretization of the PHT is a faithful representation. Since only the presence and dimension of filtration events are used (and not birth/death pairing information), this yields a faithful discretization of *any* dimension-returning transform, including the BCT. With an adaptation to our edge algorithm, we also arrive at a faithful discretization for more general topological transform, including the ECCT.

In [11], we identify challenges in reconstructing plane graphs with degree two vertices using a finite number of (non-augmented) ECCs when using methods similar to the methods presented in our current paper. In ongoing work, we are investigating if the methods of this paper can be extended to using non-augmented ECCs or PDs in general simplicial complex reconstruction.

We hope to improve our running time and reduce the required number of augmented persistence diagrams. We are also investigating ways to overcome the challenges of reconstructing codimension-zero simplices that required us to include a parabolic lifting map in our oracle.

Finally, we conjecture that the bound on APDs (or other topological descriptors) needed for a faithful discretization of the PHT (or other transforms) could be vastly improved if we assume knowledge of the underlying simplicial complex. The challenge lies in proving faithfulness without using explicit reconstruction methods.

References

- [1] Robin Lynne Belton, Brittany Terese Fasy, Rostik Mertz, Samuel Micka, David L. Millman, Daniel Salinas, Anna Schenfisch, Jordan Schupbach, and Lucia Williams. Learning simplicial complexes from persistence diagrams. In *Canadian Conference on Computational Geometry*, August 2018. Also available at arXiv:1805.10716.
- [2] Robin Lynne Belton, Brittany Terese Fasy, Rostik Mertz, Samuel Micka, David L. Millman, Daniel Salinas, Anna Schenfisch, Jordan Schupbach, and Lucia Williams. Reconstructing embedded graphs from persistence diagrams. *Computational Geometry: Theory and Applications*, 2020. doi:10.1016/j.comgeo.2020.101658.
- [3] Paul Bendich, James S. Marron, Ezra Miller, Alex Pieloch, and Sean Skwerer. Persistent homology analysis of brain artery trees. *The Annals of Applied Statistics*, 10(1):198, 2016.
- [4] Leo M. Betthauser. *Topological Reconstruction of Grayscale Images*. PhD thesis, University of Florida, 2018.
- [5] Frédéric Chazal, Vin De Silva, Marc Glisse, and Steve Oudot. *The Structure and Stability of Persistence Modules*. Springer, 2016.
- [6] David Cohen-Steiner, Herbert Edelsbrunner, and Dmitriy Morozov. Vines and vineyards by updating persistence in linear time. In *Symposium on Computational Geometry*, pages 119–126. 2006. doi:http://doi.acm.org/10.1145/1137856.1137877.
- [7] Lorin Crawford, Anthea Monod, Andrew X Chen, Sayan Mukherjee, and Raúl Rabadán. Predicting clinical outcomes in glioblastoma: An application of topological and functional data analysis. *Journal of the American Statistical Association*, pages 1–12, 2019.
- [8] Justin Curry, Sayan Mukherjee, and Katharine Turner. How many directions determine a shape and other sufficiency results for two topological transforms. arXiv:1805.09782, 2018.
- [9] Cecil Jose A. Delfinado and Herbert Edelsbrunner. An incremental algorithm for Betti numbers of simplicial complexes. In *Symposium on Computational geometry*, pages 232–239, 1993.

- [10] Herbert Edelsbrunner and John Harer. *Computational Topology: An Introduction*. American Mathematical Society, 2010.
- [11] Brittany Terese Fasy, Samuel Micka, David L Millman, Anna Schenfisch, and Lucia Williams. Challenges in reconstructing shapes from Euler characteristic curves. 2018. arXiv:1811.11337.
- [12] Brittany Terese Fasy, David Millman, and Anna Schenfisch. A total order on and lower bound representation of common topological descriptors. Unpublished manuscript (will be posted on ArXiv by SoCG camera-ready deadline), 2020.
- [13] Robert Ghrist, Rachel Levanger, and Huy Mai. Persistent homology and Euler integral transforms. *Journal of Applied and Computational Topology*, 2(1-2):55–60, 2018.
- [14] Chad Giusti, Eva Pastalkova, Carina Curto, and Vladimir Itskov. Clique topology reveals intrinsic geometric structure in neural correlations. *Proceedings of the National Academy of Sciences*, 112(44):13455–13460, 2015.
- [15] Christoph Hofer, Roland Kwitt, Marc Niethammer, Yvonne Höller, Eugen Trinka, and Andreas Uhl. Constructing shape spaces from a topological perspective. In *International Conference on Information Processing in Medical Imaging*, pages 106–118. Springer, 2017.
- [16] Qitong Jiang, Sebastian Kurtek, and Tom Needham. The weighted Euler curve transform for shape and image analysis. In *Proceedings of the IEEE/CVF Conference on Computer Vision and Pattern Recognition Workshops*, pages 844–845, 2020.
- [17] Peter Lawson, Andrew B Sholl, J Quincy Brown, Brittany Terese Fasy, and Carola Wenk. Persistent homology for the quantitative evaluation of architectural features in prostate cancer histology. *Scientific Reports*, 9, 2019.
- [18] Yongjin Lee, Senja D. Barthel, Paweł Dłotko, S. Mohamad Moosavi, Kathryn Hess, and Berend Smit. Quantifying similarity of pore-geometry in nanoporous materials. *Nature Communications*, 8:15396, 2017.
- [19] Clément Maria, Steve Oudot, and Elchanan Solomon. Intrinsic Topological Transforms via the Distance Kernel Embedding. In Sergio Cabello and Danny Z. Chen, editors, *36th International Symposium on Computational Geometry (SoCG 2020)*, volume 164 of *Leibniz International Proceedings in Informatics (LIPIcs)*, pages 56:1–56:15, Dagstuhl, Germany, 2020. Schloss Dagstuhl–Leibniz-Zentrum für Informatik. doi:10.4230/LIPIcs.SoCG.2020.56.
- [20] Alexander McCleary and Amit Patel. Edit distance and persistence diagrams over lattices. *arXiv 2010.07337*, 2020.
- [21] Samuel Adam Micka. *Searching and Reconstruction: Algorithms with Topological Descriptors*. PhD thesis, Montana State University, 2020.
- [22] Abbas H. Rizvi, Pablo G. Camara, Elena K. Kandror, Thomas J. Roberts, Ira Schieren, Tom Maniatis, and Raul Rabadan. Single-cell topological RNA-seq analysis reveals insights into cellular differentiation and development. *Nature Biotechnology*, 35(6):551, 2017.
- [23] Gurjeet Singh, Facundo Mémoli, and Gunnar E Carlsson. Topological methods for the analysis of high dimensional data sets and 3d object recognition. *SPBG*, 91:100, 2007.
- [24] L.N. Trefethen and D. Bau. *Numerical Linear Algebra*. Society for Industrial and Applied Mathematics, 1997.
- [25] Katharine Turner, Sayan Mukherjee, and Doug M. Boyer. Persistent homology transform for modeling shapes and surfaces. *Information and Inference: A Journal of the IMA*, 3(4):310–344, 2014.
- [26] Sarah Tymochko, Elizabeth Munch, Jason Dunion, Kristen Corbosiero, and Ryan Torn. Using persistent homology to quantify a diurnal cycle in hurricanes. *Pattern Recognition Letters*, 2020.

- [27] Yuan Wang, Hernando Ombao, and Moo K Chung. Statistical persistent homology of brain signals. In *IEEE International Conference on Acoustics, Speech and Signal Processing (ICASSP)*, pages 1125–1129. IEEE, 2019.

A Augmented Descriptors are Well-Defined

In this appendix, we formally define the augmented persistence diagram and the augmented Euler characteristic curve.

A.1 APDs are Well-Defined

The augmented persistence diagram (APD) is well-defined. That is, that Definition 1 is independent of the choice of the ordering of the simplices in the index filtration.

Lemma 25 (APD is Well-Defined). *Let K be a simplicial complex, and let $f: K \rightarrow \mathbb{R}$ be a monotonic function. Then, the augmented persistence diagram $\widehat{\mathcal{D}}(f)$ is well-defined.*

Proof. For $t \in \mathbb{N}$, let $f_t: K \rightarrow \mathbb{N}$ be all filter functions compatible with f ordered such that either and f_{t+1} are either same function ($f_t = f_{t+1}$), or they agree except for one transposition for each. As in Equation (2), define the following multisets:

$$\mathcal{A}_t := \{(f(\sigma_i), f(\sigma_j))\}_{(i,j) \in \mathcal{D}_k(f_t)}$$

We prove by induction that $\mathcal{A}_t = \mathcal{A}_1$ for each $t \in \mathbb{N}$. The base case is straightforward: $\mathcal{A}_1 = \mathcal{A}_1$. For the inductive assumption, let $t \geq 1$ and assume that $\mathcal{A}_t = \mathcal{A}_1$. If $f_t = f_{t+1}$, we are done. Otherwise, f_t and f_{t+1} differ by one transposition. Thus, there exists $\sigma_t, \sigma'_t \in K$, where $f_t(\sigma_t) = f_{t+1}(\sigma_t) - 1$ and $f_t(\sigma'_t) = f_{t+1}(\sigma'_t) + 1$, and $f_t(\sigma) = f_{t+1}(\sigma)$ for all other $\sigma \in K$. Since f_t is compatible with f , we know that $f(\sigma) \leq f(\sigma')$. Since f_{t+1} is also compatible with f , we know that $f(\sigma') \leq f(\sigma)$. Hence, $f(\sigma) = f(\sigma')$.

Note that the persistence diagrams $\mathcal{D}_k(f_t)$ and $\mathcal{D}_k(f_{t+1})$ induce matchings on K . By [6], there are three cases where the matchings can change: (1) two birth events swap; (2) two death events swap; (3) a birth event and a death event swap. In all three cases, the pairing swaps correspond to σ and σ' . Since $f(\sigma) = f(\sigma')$, we have $\mathcal{A}_{t+1} = \mathcal{A}_t$. \square

A.2 (Augmented) Betti Curves

Although this paper is written in the language of the PHT, the results hold for a large class of topological transforms, including the Betti Curve Transform (BCT). The k^{th} Betti number of a simplicial complex K is the rank of the k -dimensional homology group of K , and is denoted $\beta_k(K) = \text{rank}(H_k(K))$. Measuring this quantity as a filtration parameter changes gives rise to the k^{th} Betti curve, and the set of all curves for all $k \in \mathbb{Z}$ is collectively referred to as the *Betti curves*.

Definition 26 (Betti Curve (BC) and Augmented BC). *Given a filter $f: K \rightarrow \mathbb{R}$, let f' be a compatible index filtration. Let $T = \{t_1, t_2, \dots, t_\eta\}$ be the ordered set of filter parameters of f that witness a change in homology. The k^{th} Betti curve (k^{th} BC) is a step function $\beta_{f,k}: \mathbb{R} \rightarrow \mathbb{Z}$ defined by the following:*

$$\beta_{f,k} := \{\beta_k(p), p \in [t_i, t_{i+1})\}$$

Furthermore, we write $\sigma_i \in K_k$ to be the simplex such that $f'(\sigma_i) = i$. The k^{th} augmented Betti curve (k^{th} ABC) is the decorated step function $\widehat{\beta}_{f,k}: \mathbb{R} \rightarrow \mathbb{Z}$ defined by

$$\widehat{\beta}_{f,k} = \{\beta_k(p), p \in [f(\sigma_i), f(\sigma_j))\},$$

where $(i, j]$ is an interval with constant value in the function $\beta_{f',k}$. Note that some $[f(\sigma_i), f(\sigma_j))$ will be empty, so the recorded Betti number takes place at a single point rather than an interval with positive measure. It is these extra points that “decorate” the otherwise regularly defined step function. Then, the ABC represents the BC as a parameterized count of k -simplices.

We can read off the BC from the PD by observing the following equality:

$$\widehat{\beta}_{f,k}(p) = \left| \{(a, b) \in \widehat{\mathcal{D}}_k(f) \text{ s.t. } a \leq p \text{ and } b \geq p\} \right|$$

In other words, the BC is a weaker invariant than the PD. Similarly, the ABC is a weaker invariant than the APD; we further explore the relationship between these and other descriptors in [12]. Next, we observe that ABCs are dimension-returning.

Corollary 27 (Properties of ABCs). *Let $f: K \rightarrow \mathbb{R}$ be a monotonic function. For each $\sigma \in K$, the collection of functions $\{\widehat{\beta}_{f,k}\}_{k \in \mathbb{Z}}$ records the value $f(\sigma)$ and dimension of σ .*

Next, we provide an explicit definition of the BCT and make our final observation.

Definition 28 (Betti Curve Transform). *Given a geometric simplicial complex $K \in \mathbb{R}^d$, the Betti Curve Transform (BCT) of K is the set of all directional ABCs of lower-star filtrations over K , parameterized by the sphere of directions, \mathbb{S}^{d-1} .*

Thus, since the BCT is a dimension-returning transform, the the discretization developed in the body of the paper can also serve as a discretization of the BCT.

A.3 (Augmented) Euler Characteristic Curves

In this section, we show how our algorithm can be adapted to a more general class of topological descriptors, including the Euler Characteristic Curve Transform (ECCT). The Euler characteristic of a simplicial complex is the alternating sum of the number of simplices of different dimensions: $\chi(K) = \sum_{i=0}^{\kappa} (-1)^i n_i$, where we recall that n_i is the number of i -dimensional simplices in K and $\kappa = \dim(K)$. Given a filtration, the Euler characteristic with respect to the filtration parameter is known as the Euler Characteristic curve (ECC). Formally,

Definition 29 (Euler Characteristic Curve (ECC) and Augmented ECC). *Given a filter $f: K \rightarrow \mathbb{R}$, let f' be a compatible index filtration. Let $\{F_i := f^{-1}(-\infty, t_i]\}_{i=1}^n$ be the filtration of K with respect to f , as in Equation (1). The Euler characteristic curve is a step function $\chi_f: \mathbb{R} \rightarrow \mathbb{Z}$ defined by the following equation:*

$$\chi_f(p) := \sum_{k=0}^{\infty} (-1)^k n_k^{(i)}, \quad (17)$$

where $p \in [t_i, t_{i+1})$ and $n_k^{(i)}$ is the number of k -simplices in F_i . Furthermore, the augmented Euler characteristic curve (AECC) is the function $\widehat{\chi}_f: \mathbb{R} \rightarrow \mathbb{Z}^2$ defined by

$$\widehat{\chi}_f(p) = \left(\sum_{k=0}^{\infty} n_{2k}^{(i)}, \sum_{k=0}^{\infty} n_{2k+1}^{(i)} \right)$$

In other words, the AECC represents the ECC as a parameterized count of positive (even parity) and negative (odd parity) simplices.

We can read off the ECC from the PD, and the AECC from the APD. In other words, the ECC is a weaker invariant than the PD and the AECC is a weaker invariant than the APD; we further explore the relationship between these and other descriptors in [12].

Remark 30 (From Persistence Diagrams to ECCs). *Let $f: K \rightarrow \mathbb{R}$ be a monotonic function. Let $\{t_i\}_{i=1}^{\eta}$ be the set of event times, and let $p \in [t_i, t_{i+1})$. Then, the following holds:*

$$\chi_f(p) = \sum_{k \in \mathbb{Z}} \sum_{\substack{(a,b) \in \mathcal{D}_k(f) \\ a \leq p < b}} (-1)^k$$

For each $p \in \mathbb{R}$, let $A_k(p) := \{(a, b) \in \widehat{\mathcal{D}}_{k-1}(f) \text{ s.t. } b \leq p\} \cup \{(a, b) \in \widehat{\mathcal{D}}_k(f) \text{ s.t. } a \leq p\}$. Then,

$$\widehat{\chi}_f(p) = \left(\sum_{\substack{k \in \mathbb{Z} \\ k \text{ even}}} |A_k(p)|, \sum_{\substack{k \in \mathbb{Z} \\ k \text{ odd}}} |A_k(p)| \right).$$

Corollary 31 (Properties of AECCs). *Let $f: K \rightarrow \mathbb{R}$ be a monotonic function. For each $\sigma \in K$, the function $\hat{\chi}_f$ records the value $f(\sigma)$ and the parity of $\dim(\sigma)$.*

B Subroutines and Proofs for Edge Reconstruction

In the following appendix, we provide details of algorithms, lemmas, and theorems that were omitted from Section 3.3.

B.1 Details of Algorithm 8 (SplitInterval)

Algorithm 8 splits a given edge interval object \mathbf{eI} into two edge intervals, each covering half as many vertices of K (here, recall that $\mathbf{eI}.\mathbf{verts}$ are the set of “consecutive” vertices such that $\mathbf{eI}.\mathbf{count}$ of them are adjacent to $\mathbf{eI}.\mathbf{v}$). We split the set $\mathbf{eI}.\mathbf{verts}$ in half by choosing a direction s in the (b_1, b_2) -plane such that half of the vertices in $\mathbf{eI}.\mathbf{verts}$ are above v and half are below in direction s ; specifically, in Line 2, we choose

$$s = e^{\frac{1}{2}i(2\alpha - \pi - \theta)} = \left(\cos\left(\alpha - \frac{1}{2}\pi - \frac{1}{2}\theta\right), \sin\left(\alpha - \frac{1}{2}\pi - \frac{1}{2}\theta\right), 0, 0, \dots, 0 \right), \quad (18)$$

where $\alpha \in [0, \pi]$ is the angle between b_1 and the vector from $\mathbf{eI}.\mathbf{v}$ to the middle vertex in $\mathbf{eI}.\mathbf{verts}$ when projected into the (b_1, b_2) -plane. (In the case that $\mathbf{eI}.\mathbf{verts}$ has an even number of vertices, we have two candidates for the middle vertex. Choose the one with the lower index). Finally, the two new edge interval objects are created by splitting the set of vertices in $\mathbf{eI}.\mathbf{verts}$ in half in Lines 5 and 6. See Figure 2 for a demonstration of two calls to the algorithm.

Algorithm 8 SplitInterval(\mathbf{eI}, E, θ)

Input: \mathbf{eI} , an edge interval; E , an array of vertices adjacent to $\mathbf{eI}.\mathbf{v}$ but not in $\mathbf{eI}.\mathbf{verts}$ sorted cw about $\pi_{1,2}(\mathbf{eI}.\mathbf{v})$; θ , the smallest angle between any lines defined by $\mathbf{eI}.\mathbf{verts}$; and $K_0 \setminus \{\mathbf{eI}.\mathbf{v}\}$

Output: \mathbf{eI}_ℓ and \mathbf{eI}_r , edge intervals satisfying the properties in Lemma 10

- 1: Set α to be the angle between b_1 and the vector from $\pi_{1,2}v_2$ to the projected middle vertex in $\mathbf{eI}.\mathbf{verts}$
 - 2: $s \leftarrow e^{\frac{1}{2}i(2\alpha - \pi - \theta)}$
 - 3: $|E_\ell| \leftarrow$ number of vertices in E that are below $\mathbf{eI}.\mathbf{v}$ in direction s
 - 4: $|E_r| \leftarrow$ number of vertices in E that are above $\mathbf{eI}.\mathbf{v}$ in direction s
 - 5: Create edge interval \mathbf{eI}_ℓ centered at \mathbf{v} with $\mathbf{count} = \text{ComputeIndegree}(v, s, 1) - |E_\ell|$ and \mathbf{verts} the first half of the vertices in $\mathbf{eI}.\mathbf{verts}$.
 - 6: Create edge interval \mathbf{eI}_r centered at \mathbf{v} with $\mathbf{count} = \text{ComputeIndegree}(v, -s, 1) - |E_r|$ and \mathbf{verts} the second half of the vertices in $\mathbf{eI}.\mathbf{verts}$.
 - 7: **return** $(\mathbf{eI}_\ell, \mathbf{eI}_r)$
-

We next prove the correctness and runtime of Algorithm 8 in the following lemma, originally stated in Section 3.3.

Lemma 10 (Interval Splitting). *Let $K \subset \mathbb{R}^d$ be a simplicial complex, $v \in K_0$ a vertex, and \mathbf{eI} an edge interval. Then, Algorithm 8 uses two diagrams and $\Theta(n_0^2 + \Pi)$ time to split \mathbf{eI} into two new edge intervals \mathbf{eI}_ℓ and \mathbf{eI}_r with the properties:*

- (i) *The vertex sets $\mathbf{eI}_r.\mathbf{verts}$ and $\mathbf{eI}_\ell.\mathbf{verts}$ partition $\mathbf{eI}.\mathbf{verts}$ into the two sets of vertices, above and below $\mathbf{eI}.\mathbf{v}$ in direction s defined on Line 2.*
- (ii) *The new edge interval objects each contain at most half of the vertices of the original edge object.*
- (iii) *The new edge objects contain the correct edge counts; that is, $\mathbf{eI}_\ell.\mathbf{count} = |\{v' \in \mathbf{eI}_\ell.\mathbf{verts} \text{ s.t. } (v, v') \in K_1\}|$ and $\mathbf{eI}_r.\mathbf{count} = |\{v' \in \mathbf{eI}_r.\mathbf{verts} \text{ s.t. } (v, v') \in K_1\}|$.*

Proof. We first show Parts (i) and (ii) Let $i = \lfloor \frac{1}{2}|\mathbf{eI}.\mathbf{verts}| \rfloor$, and recall that $\mathbf{eI}.\mathbf{verts} = \{v_1, v_2, \dots, v_k\}$ orders the vertices in decreasing angle with b_1 . Then, as described above, $s = e^{\frac{1}{2}i(2\alpha - \pi - \theta)}$, where $\alpha \in [0, \pi]$

is the angle the vector from $\mathbf{eI.v}$ to the v_i makes with b_1 . Let $s' = e^{\frac{1}{2}i(2\alpha-\pi)}$; by construction, $\mathbf{eI.v}$ and w are at the same height in direction s' and the first half of $\mathbf{eI.verts}$ excluding v_i (namely, v_1, v_2, \dots, v_{i-1}) is below $\mathbf{eI.v}$ in direction s' , and the second half of $\mathbf{eI.verts}$ (namely, $v_{i+1}, v_{i+2}, \dots, v_k$) are above $\mathbf{eI.v}$ in direction s . Since θ is the smallest angle between any two lines defined by $\mathbf{eI.v}$ and vertices in $K_0 \setminus \{\mathbf{eI.v}\}$, we know that “tilting” s' by $\frac{1}{2}\theta$ (in particular, direction s) results in a direction such that no other vertex is at the same height as $\mathbf{eI.v}$. Moreover, a vertex $v_j \in K_0 \setminus \{\mathbf{eI.v}, v_i\}$ is below (above) s if and only if it was below (above) s' . Thus, v_1, v_2, \dots, v_i are below $\mathbf{eI.v}$ in direction s and $v_{i+1}, v_{i+2}, \dots, v_k$ are above $\mathbf{eI.v}$ in direction s . Thus, Parts (i) and (ii) hold.

We now prove Part (iii) for \mathbf{eI}_ℓ and note that the proof of \mathbf{eI}_r follows the same argument. By Theorem 16, the value returned from $\text{ComputeIndegree}(v, s, 1)$ counts all edges incident to v and below $v \cdot s$ in direction s . This is exactly equal to the total number of edges in \mathbf{eI}_ℓ and edges $(v, v') \in E_v$ for which $v' \cdot s < v \cdot s$. Thus, $\mathbf{eI}_\ell.\text{count}$ is the k -indegree of v from direction s minus the number of elements in E_ℓ as in Line 3 and Part (iii) is satisfied.

For the runtime, we look at the time and diagram complexity of each line. The computation of s in Lines 1 and 2 requires: finding the middle vertex of $\mathbf{eI.verts}$; projecting $\mathbf{eI.v}$ and the middle vertex; then computing the coordinates using sin and cos as specified in Equation (18). Each of these operations is constant time, since $\mathbf{eI.verts}$ is a sorted array and we are working in the (b_1, b_2) -plane. Since E is sorted and since s has only two non-zero coordinates, we can find $|E_\ell|$ and $|E_r|$ in $\Theta(\log |E|)$ time (Lines 3 and 4). By Theorem 17(i), the two calls to $\text{ComputeIndegree}(v, \cdot, 1)$ in Lines 5 and 6 each use one diagram and run in $\Theta(n_0^2 + \Pi)$ time. These two lines also split $\mathbf{eI.verts}$ into two sets, which can be done in $\Theta(d|\mathbf{eI.verts}|)$ time by walking through $\mathbf{eI.verts}$ and storing each one explicitly, or can be done in $\Theta(\log |\mathbf{eI.verts}|)$ if we store pointers to the beginning / end of the sub-array corresponding to the \mathbf{verts} variable of the new edge interval objects. Again, computing the heights is only a constant time operation (as opposed to $\Theta(d)$), since we are working in the (b_1, b_2) -plane. Since $|E| + |\mathbf{eI.verts}| = n_0$, one of the two summands must be at least $\frac{1}{2}n_0$, which means that $\log |E| + \log |\mathbf{eI.verts}| = \Theta(\log n_0)$. Thus, the overall runtime of Algorithm 8 is $\Theta(1 + \log |E| + n_0^2 + \Pi + \log |\mathbf{eI.verts}|) = \Theta(\log n_0 + n_0^2 + \Pi) = \Theta(n_0^2 + \Pi)$, and the algorithm uses two diagrams. \square

C Codimension-Zero Reconstruction

In the following appendix, we give a straightforward extension of our main results in the case that the underlying simplicial complex contains codimension-zero simplices.

Recall that our main result is stated for $K \subset \mathbb{R}^d$ where κ , the dimension of K , is strictly less than the dimension of the embedding space, d . Here, we provide a straightforward adaptation to our results that integrates a parabolic lift that allows us to reconstruct simplicial complexes with $\kappa = d$.

To reconstruct K , we follow the same reconstruction for dimensions zero through $\kappa - 1$, which is permissible since $\kappa - 1 < d$. Then, we test for κ simplices using the lifted oracle, which we will define next.

First, we define the lifting map \mathcal{L} that takes a simplicial complex in \mathbb{R}^d to a simplicial complex in \mathbb{R}^{d+1} by mapping vertex $v = (v^{(1)}, v^{(2)}, \dots, v^{(d)}) \in K$ to $(v^{(1)}, v^{(2)}, \dots, v^{(d)}, v \cdot v)$; all higher-dimensional simplices follow. Then, we define the lifted oracle $\text{Oracle}_\uparrow(s, i)$ that takes direction $s \in \mathbb{R}^{d+1}$ and dimension $i \in \mathbb{Z}$ and returns the dimension- i APD of $\mathcal{L}(K)$. We define IsLiftedSimplex similar to IsSimplex , however, we replace all calls to Oracle with Oracle_\uparrow . The following is a direct result of Theorem 19.

Corollary 32 (Lifted Simplex Predicate). *Let $K \subset \mathbb{R}^d$ be a simplicial complex $\sigma \in K_{d-1}$, and $v \in K_0 \setminus \text{verts}(\sigma)$. Then, $\text{IsLiftedSimplex}(\sigma, v)$ returns *True* iff $\text{verts}(\sigma) \cup \{v\}$ defines a d -simplex in K in time $O(2^d nn_0(nn_0 + d^2 + 2^d + \Pi) + dnn_0^2 + d\Pi)$ with $O(nn_0 2^d)$ diagrams.*

Proof. This proof closely follows the proof of Theorem 21, since Algorithm 9 is a slight modification of Algorithm 7. Indeed, we can account for the extra work in Lines 9–11, by rewriting each summation in Equations (10)–(14) with an upper bound of d , which results in a running time of $O(2^d nn_0(nn_0 + d^2 + 2^d + \Pi) + dnn_0^2 + d\Pi)$. Similarly, we can account for the extra diagrams by rewriting Equation (16) with an upper bound of d , which results in $O(nn_0 2^d)$ APDs. \square

The following algorithm is nearly identical to Algorithm 7, but contains the described modification. Specifically, to identify d -simplices, it makes calls to IsLiftedSimplex rather than IsSimplex .

Algorithm 9 CodimZeroReconstruct()

Input: none (but makes calls to global **Oracle** and **Oracle_↑**)

Output: the reconstructed simplicial complex

```
 $K_0 \leftarrow \text{FindVertices}()$  ▷ Algorithm 2  
 $K_1 \leftarrow \text{FindEdges}(K_0)$  ▷ Algorithm 4  
for  $i \in \{2, 3, \dots, d-1\}$  do  
  for  $\sigma \in K_{i-1}$  do  
    for  $v \in K_0 \setminus \text{verts}(\sigma)$  do  
      if IsSimplex( $\sigma, v$ ) then  
        Add  $\sigma \cup \{v\}$  to  $K_i$   
for  $\sigma \in K_{d-1}$  do  
  for  $v \in K_0 \setminus \text{verts}(\sigma)$  do  
    if IsLiftedSimplex( $\sigma, v$ ) then  
      Add  $\sigma \cup \{v\}$  to  $K_d$   
return  $K_0 \cup K_1 \cup \dots \cup K_d$ 
```

Note that Algorithm 9 could be used in the case that $\kappa < d$. The result would be that in iterations after κ , the set of lower dimensional simplices would be empty and so the algorithm would not evaluate the inner loops or check for simplices.